COMENIUS UNIVERSITY IN BRATISLAVA
FACULTY OF MATHEMATICS, PHYSICS AND INFORMATICS

Analysis of model of cell death in presence of invasion by Trichinella Spiralis parasite

MASTER THESIS

2016 Bc. Peter Barančok

COMENIUS UNIVERSITY IN BRATISLAVA
FACULTY OF MATHEMATICS, PHYSICS AND INFORMATICS
DEPARTMENT OF APPLIED MATHEMATICS AND STATISTICS

Analysis of model of cell death in presence of invasion by Trichinella Spiralis Parasite

MASTER THESIS

Study programme:	Mathematical Economics, Finance and Modelling
Branch of study:	9.1.9 Applied mathematics
Departement:	Department of Applied Mathematics and Statistics
Supervisor:	doc. Mgr. Richard Kollár, PhD

Bratislava 2016 **Bc. Peter Barančok**

Comenius University in Bratislava
Faculty of Mathematics, Physics and Informatics

THESIS ASSIGNMENT

Name and Surname:	Bc. Peter Barančok
Study programme:	Mathematical Economics, Finance and Modelling (Single degree study, master II. deg., full time form)
Field of Study:	Applied Mathematics
Type of Thesis:	Diploma Thesis
Language of Thesis:	English
Secondary language:	Slovak

Title: Analysis of model of cell death in presence of invasion by Trichinella Spiralis parasite

Aim: The goal of the thesis is an analysis of the model of programmed cell death (apoptosis) in cells invaded by Trichinella Spiralis proposed by Jakub Kovács in his diploma thesis (FMFI UK, 2014).

Supervisor:	Mgr. Richard Kollár, PhD.
Department:	FMFI.KAMŠ - Department of Applied Mathematics and Statistics
Head of department:	prof. RNDr. Daniel Ševčovič, CSc.
Assigned:	10.02.2015

Approved: 11.02.2015 prof. RNDr. Daniel Ševčovič, CSc.
Guarantor of Study Programme

.....
Student

.....
Supervisor

Acknowledgement I would like to express my gratitude and appreciation to my supervisor doc. Mgr. Richard Kollár, PhD. for his guidance and support throughout the elaboration of this thesis.

Abstrakt

Barančok, Peter: Analýza modelu bunkovej smrti v prítomnosti invázie parazitom Trichinella Spiralis [Diplomová práca], Univerzita Komenského v Bratislave, Fakulta matematiky, fyziky a informatiky, Katedra aplikovanej matematiky a štatistiky; školiteľ: doc. Mrg. Richard Kollár, PhD., Bratislava, 2016.

Apoptóza, alebo riadená bunková smrť, je bežne sa vyskytujúci proces vo všetkých mnohobunkových organizmoch nevyhnutná pre zachovanie homeostatickej rovnováhy medzi delením a zánikom buniek. Je tiež dôležitým obranným mechanizmom organizmov pred poruchami správneho fungovania buniek, ktoré môžu nastať ako dôsledok rôznych, či už vnútorných alebo vonkajších, podnetov. Pre svalové bunky je jedným z takýchto podnetov práve invázia larvy parazita Trichinella spiralis. V tejto práci analyzujeme dva matematické modely navrhnuté v diplomovej práci Jakuba Kovácsa. Navrhneme niekoľko zmien aby lepšie zachytával biochemické procesy prebiehajúce v bunkách počas apoptózy a rozšírime model tak, aby zahrňoval aj proces fragmentácie DNA a jej vplyvu na syntézu proteínov zúčastňujúcich sa na regulácií apoptózy. Nakoniec výrazne zredukujeme veľkosť modelu pri zachovaní jeho kvalitatívneho správania.

Kľúčové slová: matematické modelovanie, apoptóza, Trichinella spiralis, mitochondrie

Abstract

Barančok, Peter: Analysis of model of cell death in presence of invasion by Trichinella Spiralis parasite [Master Thesis], Comenius University in Bratislava, Faculty of Mathematics, Physics and Informatics, Department of Applied Mathematics and Statistics; Supervisor: doc. Mrg. Richard Kollár, PhD., Bratislava, 2016.

Apoptosis, or programmed cell death, is a natural process in all multicellular organisms essential in maintaining homeostatic balance between cell proliferation and death. It is also an important defence mechanism for protection of an organism from malfunctions arising from cell stress or damage induced by various, internal or external, stimuli. For muscle cell one such stimulus is the invasion of Trichinella spiralis parasite. In this thesis we analyse two mathematical models of apoptosis in presence of a synchronous invasion of Trichinella spiralis proposed in Jakub Kovács's master thesis. Also, we propose a few modifications to the model to better model biochemical processes taking place in cells during apoptosis and to expand the model to incorporate process of DNA fragmentation during apoptosis and its effect on synthesis of proteins involved in the apoptotic regulatory pathway. Finally we significantly reduce the dimension of the model while preserving its qualitative behaviour.

Keywords: mathematical modelling, apoptosis, Trichinella spiralis, mitochondria

Contents

Introduction

Apoptosis is the process of programmed cell death and is the naturally occuring process in all multicellular organisms essential in maintaining homeostatic balance between cell proliferation and death. It is also an important defence mechanism for protection of organism from malfunctions arising from cell stress or damage induced by various, internal or external, stimuli. Many researchers are highly interested in apoptosis nowadays as it plays significant role in several diseases. Insufficient apoptotic activity gives rise to uncontrolled cell growth and cancer, while hypersensitivity to even small apoptotic signals cause muscle atrophy and neurodegenerative disorders such as Alzheimer's and Parkinson's diseases.

Trichinella spiralis is an intracellular parasite infecting mammalian (e.g. pig's, rodent's, bear's and human's) muscle cells, but unlike the majority of intracellular parasites, it occupies the host muscle cell without destroying it. Invasion into muscle cell triggers apoptosis that should kill the cell and parasite, however, Trichinella spiralis is able to use apoptosis to remodel muscle cell into the nurse cell.

In today's computer age, mathematical modelling and computer simulations represent powerful tools that can increase or insight into the mechanisms of biological processes. Realistic mathematical models provide increasingly useful alternative to the experiments for testing hypotheses and making predictions about effects of the experimental treatments.

In this thesis we conduct qualitative analysis of several mathematical models of apoptosis in the presence of Trichinella spiralis. Also we incorporate DNA fragmentation that is caused during apoptosis by apoptosis inducing factor, AIF, and caspase-activated DNase, CAD, and its effect on synthesis of proteins involved in apoptotical signalling pathways to mathematical model proposed in [23]. And then reduce the dimension of the system that describe reactions involved in apoptotical signalling.

1 Apoptosis

Apoptosis is the process of programmed cell death and is the naturally occuring process in all multicellular organisms essential in maintaining homeostatic balance between cell proliferation and death, during embryonic development (e.g. finger separation) and for eliminating pathogen-invaded cells and cells with severly damaged DNA.

Apoptosis is regulated by the two types of apoptotic pathways: extrinsic and intrinsic. With a crosstalk between the two. Intrinsic, or mitochondrial, apoptotic pathway is activated in respose to variety of intracellular stimuli, e.g. excessive amount of calcium within the cell, oxidative stress and DNA damage.

In case of extrinsic pathways, apoptosis is initiated by extrcellular signals. Death ligands such as Fas ligand or tumour necrosis factor, bind to associated TNF-Receptors and induce oligomerisation followed by the recruitment of adaptor proteins to the cytoplasmic portions of the receptors ([29]) which results in in formation of Death Inducing Signalling Complex (DISC). DISC than recruits and bring to close proximity multiple procaspase-8 molecules that activate one another. Next development depends on the type of cell. In Type I cells caspase-8 is activated in large quantities which lead to activation cascade of caspases independently of mitochondria.

In the contrast, Type II cells only small amount of caspase-8 is activated at DISC, so apoptotic signal is amplified via the mitochondria by cleaving BH3-only protein of Bcl-2 family that promotes oligomerisation of pro-apoptotic proteins Bax and Bak of Bcl-2 family. Bax and Bak forms pores in mitochondrial outer membrane through which cytochrome c and other pro-apoptotic proteins are released. Anti-apoptotic members of Bcl-2 family such as Bcl-2 and Bcl-x_L inhibit permeabilisation of mitochondrial outer membrane by binding to Bax and Bak. Once in cytoplasm, cytochrome c binds to Apoptotic protease activating factor-1, Apaf-1, to form heptameric complex termed apoptosome that can activate procaspase-9 to caspase-9 in the similar manner as DISC activates. Caspase-9 the initiates caspase cascade.

In both types of cells caspase cascade ultimately leads to activation of caspase-3 that promotes DNA fragmentation by activation of caspase-activated DNase.

2 Trichinella spiralis

Trichinella spiralis is an intracellular parasite infecting mammalian (e.g. pig's, rodent's, bear's and human's) skeletal muscle cells, but unlike the majority of intracellular parasites, it occupies the host muscle cell without destroying it. Trichinella spiralis resides in cysts within the muscle tissue. When infected meat is consumed larvae that were in the meat mature and mate in small intestine. Newborn larvae pass through the epithelial cells of small intestine and enter the blood stream and from where invade muscle cells.

Interestingly, there is no evidence of damage done to the intestine epithelial cells, even thou infected muscle cells show expression of pro-apoptotic proteins shortly after invasion by Trichinella spiralis [5, 8]. Another phenomenon that was observed in was swelling and disappearance of mitochondria [8].

Since damage of the cell membrane structure is one of the most common pathological stimuli that initiate a cascade of suicidal intracellular processes [13], penetration of larva of Trichinella spiralis parasite thorough the muscle cell membrane does not result of the host cell's extinction. From observed similarity between muscle cell repair mechanism and nurse cell formation [43] and from passing through intestinal epithelial cells without damaging them, it can be hypothesised that Trichinella spiralis triggers apoptosis to damage muscle cell in order to hijack repair mechanisms to accomodate itself.

3 Reduced Model of Apoptosis

3.1 Modifications

First we propose few modifications to the mathematical model of apoptosis proposed in [23, Chapter 3] to more accurately describe biochemical processes that take place in cells during apoptosis induced by invasion of Trichinella spiralis.

Synthesis of Bax protein

Bax is a pro-apoptotic member of the Bcl-2 family of proteins that is an essential effector responsible for the permeabilisation of the mitochondrial outer membrane. In reduced model of apoptosis proposed in [23, Chapter 3] synthesis of Bax was dependent on the portion of active mitochondria (mit) suggesting that Bax is predominantly associated with the mitochondrial outer membrane in proliferating cells. However, according to [21] Bax in healthy cells is mainly localised in cytosol with a minor fraction loosely attached to the mitochondrial outer membrane. Under normal circumstances Bax constantly travels from the cytoplasm to mitochondria from where it is translocated to the cytosol by Bcl-x_L (see [14]), an anti-apoptotic protein from the Bcl-2 family, to prevent accumulation and possibly its autoactivation. Therefore we modify reduced model so that synthesis of Bax is independent of mitochondria. Also we omit term $r_{mito}[mit][Bax]$ from the ordinary differential equation for the concentration of Bax as it is not stored in mitochondria.

Formation of Bax_2 channels

In reduced model proposed in [23, Chapter 3] formation of Bax_2 channels is modelled using following one-step kinetic reaction scheme:

$$tBid + 2Bax \xrightarrow{k_2} tBid + Bax_2, \tag{3.1}$$

where k_2 is the corresponding reaction rate. This, however, together with the independent synthesis of Bax from mitochondria, yields physically impossible behaviour as there are still Bax_2 channels being formed even after all mitochondria have disappeared (see Figure 1; results were obtained by numerical simulation of reduced model proposed in [23, Chapter 3] with changed synthesis of Bax protein using `ode45` function form

MATLAB® software). Therefore we change the kinetic reaction scheme (4.2) to

$$tBid + 2Bax + mit \xrightarrow{k_2} tBid + Bax_2 + mit. \tag{3.2}$$

to accommodate effect of disappearance of mitochondria into dynamics of Bax_2 channels formation.

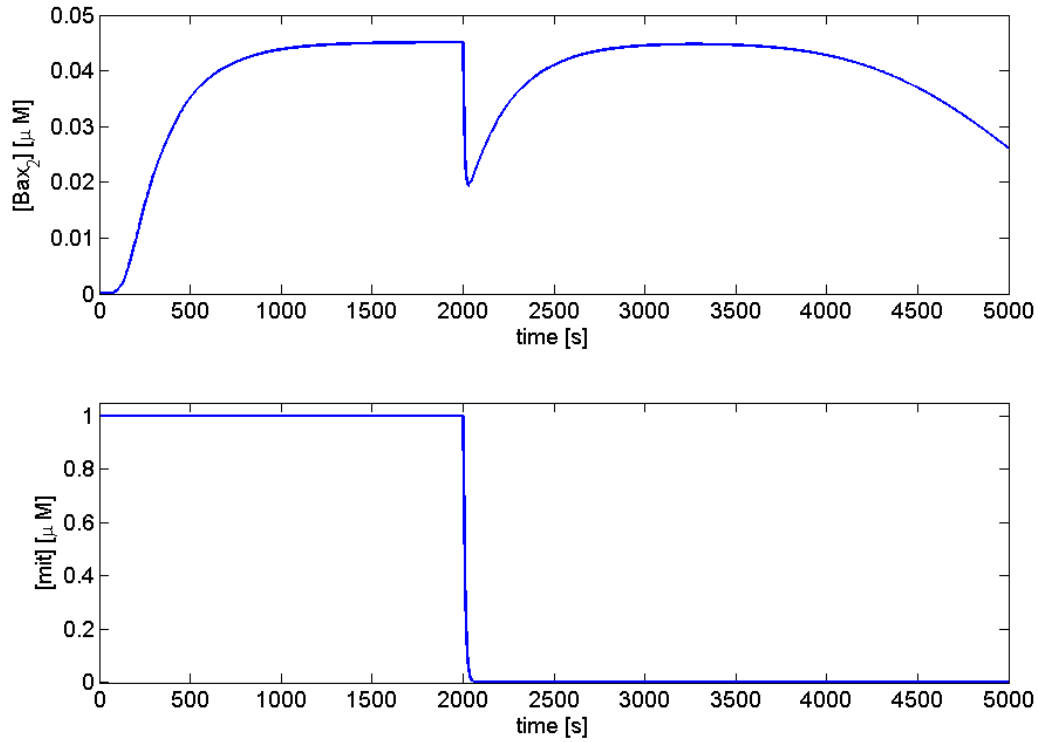

Figure 1: Evolution of concentration of Bax_2 (left) and portion of active mitochondria (right). Mitochondria started disappearing at time $t = 2000\,\mathrm{s}$ at a rate $r_{mito} = 0.1\,\mathrm{s}^{-1}$.

3.2 Description of the model

The reduced model of apoptosis as proposed in [23, Chapter 3] consists only of the few key components (Figure 2) with simplified interactions, compared to the "full" model proposed in [23, Chapter 4]. It can be summarised by the following biochemical reactions, where k-s are the corresponding kinetic reaction rates as used in the simulations:

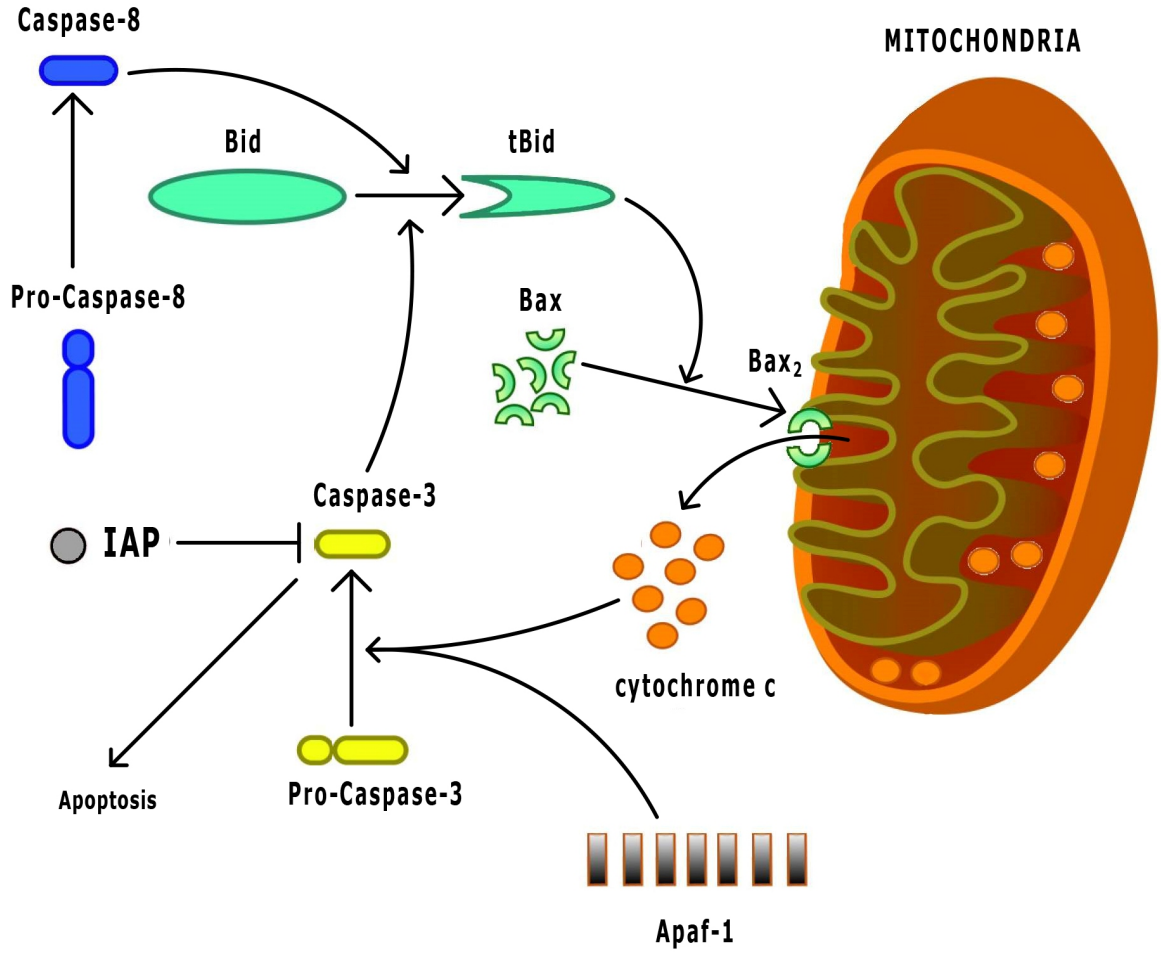

Figure 2: Graphic representation of the reduced model of apoptosis (compare to [23, Fig. 6])

Cleavage of Bid by caspase-8

Active caspase-8, $C8$ cleaves BH3-only protein Bid from the Bcl-2 family to its pro-apoptotically active truncated form $tBid$ [25, 27].

$$C8 + Bid \xrightarrow{k_1} C8 + tBid \qquad k_1 = 10\,\mu\mathrm{M}^{-1}\mathrm{s}^{-1}$$

Formation of Bax_2 channels in mitochondrial membrane

For simplicity, it is assumed that reactions occur in the close proximity of mitochondria, i.e. excluding reaction for translocation of $tBid$ onto mitochondrial outer membrane. However, mitochondria still need to be present in reaction describing formation of Bax_2 channels [21, 40, 41], otherwise it would lead to behaviour that is not biologically accurate (see section 3.1).

$$tBid + 2Bax + mit \xrightarrow{k_2} tBid + Bax_2 + mit \qquad k_2 = 10\,\mu\mathrm{M}^{-2}\mathrm{s}^{-1}$$

Release of cytochrome c from mitochondria to cytoplasm

After formation of Bax_2 channels, cytochrome c, c, is released from mitochondrial intermembrane space [11, 39, 40].

$$Bax_2 + c_{mito} \xrightarrow{k_3} Bax_2 + c \qquad k_3 = 10\,\mu\mathrm{M}^{-1}\mathrm{s}^{-1}$$

Activation of caspase-3

Kinetic describing activation of caspase-3, $C3$, is highly reduced compared to that in the "full" model. Although cooperativity of seven cytochrome c and $Apaf$-1 molecules is retained, activation of caspase-9 was left out.

$$7c + 7Apaf\text{-}1 + PC3 \xrightarrow{k_6} 7c + 7Apaf\text{-}1 + C3 \qquad k_6 = 6 \cdot 10^8\,\mu\mathrm{M}^{-14}\mathrm{s}^{-1}$$

Loop activation of caspase-8 by caspase-3

Active caspase-3 is able to activate initiator caspase-8 by cleaving its inactive form procaspase-8 [15, 17], serving as a positive feedback loop.

$$C3 + PC8 \xrightarrow{k_a} C3 + C8 \qquad k_a = 10\,\mu\mathrm{M}^{-1}\mathrm{s}^{-1}$$

Loop cleavage of Bid by caspase-3

In addition to caspase-8, active caspase-3 has also the ability to activate Bid by truncating it [27,35]. This is the second amplification feedback loop of the model.

$$C3 + Bid \xrightarrow{k_8} C3 + tBid \qquad k_8 = 10\,\mu\mathrm{M}^{-1}\mathrm{s}^{-1}$$

Inhibition of caspase-3 by IAP

Inhibitor of apoptosis, IAP, has the ability to inhibit active caspase-3 [17, 24, 32], while inhibitor of apoptosis itself stays active.

$$IAP + C3 \xrightarrow{k_x} IAP + C3_{inactive} \qquad k_x = 1\,\mu\mathrm{M}^{-1}\mathrm{s}^{-1}$$

Synthesis and degradation of molecules

The initial concentrations of all compounds are set to 10^{-4} and portion of active mitochondria is set to 1. All primary forms of proteins, that is $PC8$, Bid, Bax, c_{mito}, $Apaf$-1, $PC3$ and IAP are synthesized according to the following reactions with corresponding synthesis rates Ω.

$$\varnothing \xrightarrow{\Omega_{PC8}} PC8 \qquad \Omega_{PC8} = 6 \cdot 10^{-4}\,\mu\mathrm{Ms}^{-1}$$

$$\varnothing \xrightarrow{\Omega_{Bid}} Bid \qquad \Omega_{Bid} = 6 \cdot 10^{-5}\,\mu\mathrm{Ms}^{-1}$$

$$\varnothing \xrightarrow{\Omega_{Bax}} Bax \qquad \Omega_{Bax} = 5 \cdot 10^{-4}\,\mu\mathrm{Ms}^{-1}$$

$$mit \xrightarrow{\Omega_{c_{mito}}} c_{mito} \qquad \Omega_{c_{mito}} = 5 \cdot 10^{-4}\,\mu\mathrm{Ms}^{-1}$$

$$\varnothing \xrightarrow{\Omega_{Apaf\text{-}1}} Apaf\text{-}1 \qquad \Omega_{Apaf\text{-}1} = 6 \cdot 10^{-4}\,\mu\mathrm{Ms}^{-1}$$

$$\varnothing \xrightarrow{\Omega_{PC3}} PC3 \qquad \Omega_{PC3} = 6 \cdot 10^{-4}\,\mu\mathrm{Ms}^{-1}$$

$$\varnothing \xrightarrow{\Omega_{IAP}} IAP \qquad \Omega_{IAP} = 10^{-5}\,\mu\mathrm{Ms}^{-1}$$

A first order degradation kinetics with a uniform rate constant of $\mu = 0.004$ is adopted for all compounds.

In mathematical modelling of biochemical reactions, dynamical systems that describe dynamics of the reactions are derived using law of mass action. It states: *"Rate of any chemical reaction is proportional to the product of the masses of the reacting substances, with each mass raised to a power equal to the coefficient that occurs in the chemical equation."*. Thus, the above biochemical reactions translate into the following system of ordinary differential equations, where Ω_X is the production rate of the molecule X, μ is decomposition rate and is the same for all substances, and k-s are the kinetic reaction rates defined above with the related reactions:

$$[\dot{PC8}] = \Omega_{PC8} - \mu[PC8] - k_a[C3][PC8] \tag{3.3}$$

$$[\dot{C8}] = -\mu[C8] + k_a[C3][PC8] \tag{3.4}$$

$$[\dot{Bid}] = \Omega_{Bid} - \mu[Bid] - k_1[C8][Bid] - k_8[C3][Bid] \tag{3.5}$$

$$[\dot{tBid}] = -\mu[tBid] + k_1[C8][Bid] + k_8[C3][Bid] \tag{3.6}$$

$$[\dot{Bax}] = \Omega_{Bax} - \mu[Bax] - 2k_2[tBid][Bax]^2[mit] \tag{3.7}$$

$$[\dot{Bax_2}] = -\mu[Bax_2] + k_2[tBid][Bax]^2[mit] + r_{mito}[mit][Bax_2] \tag{3.8}$$

$$[\dot{c_{mito}}] = \Omega_{c_{mito}}[mit] - \mu[c_{mito}] - k_3[Bax_2][c_{mito}] + r_{mito}[mit][c_{mito}] \tag{3.9}$$

$$[\dot{c}] = -\mu[c] + k_3[Bax_2][c_{mito}] \tag{3.10}$$

$$[\dot{Apaf\text{-}1}] = \Omega_{Apaf\text{-}1} - \mu[Apaf\text{-}1] \tag{3.11}$$

$$[\dot{IAP}] = \Omega_{IAP} - \mu[IAP] \tag{3.12}$$

$$\dot{[PC3]} = \Omega_{PC3} - \mu[PC3] - k_6[c]^7[Apaf\text{-}1]^7[PC3] \tag{3.13}$$

$$\dot{[C3]} = -\mu[C3] + k_6[c]^7[Apaf\text{-}1]^7[PC3] - k_x[IAP][C3] \tag{3.14}$$

$$\dot{[mit]} = r_{mito}[mit] \tag{3.15}$$

3.3 Bistability

We redo the stability analysis of the steady states of the system of ordinary differential equations (3.3) – (3.15) that represents reduced model of apoptosis in order to determine how our modifications changed bifurcation diagram.

Steady states

First we need to find steady states of the system representing reduced mathematical model of apoptosis. System is in steady state if concentrations of all reactants do not change in time, i.e. they are produced at the same rate as they are consumed. Mathematically this corresponds to setting the time derivatives of reactants to zero. After setting all left hand sides in the system of differential equations (3.3) – (3.15) to zero we get system of algebraic equations and from it we obtain equilibrium concentrations of all compounds in terms of equilibrium concentrations of other compounds:

$$[PC8] = \frac{\Omega_{PC8}}{\mu + k_a[C3]} \qquad [C8] = \frac{\Omega_{PC8}}{\mu} - [PC8] \tag{3.16}$$

$$[Bid] = \frac{\Omega_{Bid}}{\mu + k_1[C8] + k_8[C3]} \qquad [tBid] = \frac{\Omega_{Bid}}{\mu} - [Bid] \tag{3.17}$$

$$[Bax_2] = \frac{\mu[c]}{k_3[c_{mito}]} \qquad [Bax] = \frac{\Omega_{Bax}}{\mu} - 2[Bax_2] \tag{3.18}$$

$$[c_{mito}] = \frac{\Omega_{c_{mito}}[mit]}{\mu} - [c] \qquad [c] = \frac{\Omega_{c_{mito}}[mit]}{\mu} - [c_{mito}] \tag{3.19}$$

$$[Apaf\text{-}1] = \frac{\Omega_{Apaf\text{-}1}}{\mu} \qquad [IAP] = \frac{\Omega_{IAP}}{\mu} \tag{3.20}$$

$$[PC3] = \frac{\Omega_{PC3}}{\mu + k_6[c]^7[Apaf\text{-}1]^7} \qquad [C3] = \frac{\Omega_{PC3} - \mu[PC3]}{\mu + k_x[IAP]} \tag{3.21}$$

Note that concentrations of all compounds can be expressed in the same forms as before we introduced modifications to the reduced model. Equation (3.15) has two

possible steady states: $r_{mito} = 0$ or $[mit] = 0$. Since the later leads only to behaviour without apoptosis, in the following analysis we will consider only the former and portion of active mitochondria, $[mit]$, will be parameter which we will vary to investigate bistability.

Substituting above expressions into algebraic equation we get from differential equation (3.7) leads to the following 16^{th} degree polynomial in concentration of cytochrome c:

$$\begin{aligned} 0 = {} & K^2 R_{L0} + [c](-2KJR_{L0} - \Omega_{c_{mito}} M R_{P0}[mit]) \\ & + [c]^2(J^2 R_{L0} + \mu M R_{P0}) + [c]^7(K^2 R_{L7}) \\ & + [c]^8(-2KJR_{L7} - \Omega_{c_{mito}} M R_{P7}[mit]) + [c]^9(J^2 R_{L7} + \mu M R_{P7}) \\ & + [c]^{14}(K^2 R_{L14}) + [c]^{15}(-2KJR_{L14} - \Omega_{c_{mito}} M R_{P14}[mit]) \\ & + [c]^{16}(J^2 R_{L14} + \mu M R_{P14}), \end{aligned} \tag{3.22}$$

where following substitutions were made:

$$\begin{aligned} R_{L0} &= \mu^2 P_{L0} + \mu\Omega_{PC3} P_{L1} + P_2 \Omega_{PC3}^2 & R_{P0} &= \mu^2 P_{P0} + \mu\Omega_{PC3} P_{P1} + P_2 \Omega_{PC3}^2 \\ R_{L7} &= 2\mu k_6 P_{L0} A^7 + k_6 \Omega_{PC3} P_{L1} A^7 & R_{P7} &= 2\mu k_6 P_{P0} A^7 + k_6 \Omega_{PC3} P_{P1} A^7 \\ R_{L14} &= k_6^2 P_{L0} A^{14} & R_{P14} &= k_6^2 P_{P0} A^{14} \\ P_{L0} &= k_8 k_a \Omega_{PC3}^2 + \Omega_{PC3} O N_1 & P_{P0} &= \mu^2 O^2 + k_8 k_a \Omega_{PC3}^2 + \Omega_{PC3} O N_2 \\ P_{L1} &= -2\mu k_8 k_a \Omega_{PC3} - \mu O N_1 & P_{P1} &= -2\mu k_8 k_a \Omega_{PC3} - \mu O N_2 \\ P_2 &= \mu^2 k_8 k_a \\ N_1 &= \mu k_8 + k_a L & N_2 &= \mu k_8 + k_a L + \mu k_a \\ O &= \mu + k_x \frac{\Omega_{IAP}}{\mu} & A &= \frac{\Omega_{Apaf\text{-}1}}{\mu} \\ M &= \frac{k_3 \mu^4}{k_2 \Omega_{Bid}[mit]} & L &= k_1 \frac{\Omega_{PC8}}{\mu} \\ K &= \frac{k_3 \Omega_{Bax} \Omega_{c_{mito}}[mit]}{\mu} & J &= k_3 \Omega_{Bax} + 2\mu^2 \end{aligned}$$

Again note that introduction of modifications changed polynomial only slightly, however, effect of these changes remains to be seen.

We obtain solutions of the polynomial (3.22), i.e. steady states of the system of differential equations (3.3) – (3.14) with the condition $r_{mito} = 0$, numerically using the `roots` function from MATLAB® software. Even thou all are mathematically correct

(up to an error produced by numerical methods used in `roots` function), not all of them are also biologically possible, so we exclude all steady states with negative or complex concentration of cytochrome c (we account for numerical errors using small tolerance, 10^{-5}, when checking non-negativity).

Stabillity of the steady states

Next we determine which of the steady states are stable and which are unstable. For that we compute eigenvalues of Jacobian matrix of the system of differential equations (3.3) – (3.14) with the condition $r_{mito} = 0$ and $[mit]$ as a parameter. Let us consider the system of differential equations $\frac{d\mathbf{x}}{dt} = \mathbf{F}(\mathbf{x})$, where $\mathbf{F}$ is differentiable. Then the $(i,j)^{th}$ element of Jacobian matrix J of this system is computed as $J_{i,j} = \frac{\partial F_i}{\partial x_j}$. For our system the Jacobian matrix can be written as a block matrix and has the following form:

$$\begin{bmatrix} J_{11} & 0 & 0 & 0 & 0 & J_{16} \\ J_{21} & J_{22} & 0 & 0 & 0 & J_{26} \\ 0 & J_{32} & J_{33} & 0 & 0 & 0 \\ 0 & 0 & J_{43} & J_{44} & 0 & 0 \\ 0 & 0 & 0 & 0 & J_{55} & 0 \\ 0 & 0 & 0 & J_{64} & J_{65} & J_{66} \end{bmatrix},$$

where individual blocks are:

$$J_{11} = \begin{bmatrix} -\mu - k_a[C3] & 0 \\ k_a[C3] & -\mu \end{bmatrix} \qquad J_{16} = \begin{bmatrix} 0 & -k_a[PC8] \\ 0 & k_a[PC8] \end{bmatrix}$$

$$J_{21} = \begin{bmatrix} 0 & -k_1[Bid] \\ 0 & k_1[Bid] \end{bmatrix} \qquad J_{22} = \begin{bmatrix} -k_1[C8] - k_8[C3] - \mu & 0 \\ k_1[C8] + k_8[C3] & -\mu \end{bmatrix}$$

$$J_{26} = \begin{bmatrix} 0 & -k_8[Bid] \\ 0 & k_8[Bid] \end{bmatrix} \qquad J_{32} = \begin{bmatrix} 0 & -2k_2[Bax]^2[mit] \\ 0 & k_2[Bax]^2[mit] \end{bmatrix}$$

$$J_{33} = \begin{bmatrix} -4k_2[tBid][Bax][mit] - \mu & 0 \\ 2k_2[tBid][Bax][mit] & -\mu \end{bmatrix} \qquad J_{43} = \begin{bmatrix} 0 & -k_3[c_{mito}] \\ 0 & k_3[c_{mito}] \end{bmatrix}$$

$$J_{44} = \begin{bmatrix} -k_3[Bax_2] - \mu & 0 \\ k_3[Bax_2] & -\mu \end{bmatrix} \qquad J_{55} = \begin{bmatrix} -\mu & 0 \\ 0 & -\mu \end{bmatrix}$$

$$J_{64} = \begin{bmatrix} 0 & -7k_6[PC3][Apaf\text{-}1]^7[c]^6 \\ 0 & 7k_6[PC3][Apaf\text{-}1]^7[c]^6 \end{bmatrix} \qquad J_{65} = \begin{bmatrix} -7k_6[PC3][Apaf\text{-}1]^6[c]^7 & 0 \\ 7k_6[PC3][Apaf\text{-}1]^6[c]^7 & -k_x[C3] \end{bmatrix}$$

$$J_{66} = \begin{bmatrix} -k_6[Apaf\text{-}1]^7[c]^7 - \mu & 0 \\ k_6[Apaf\text{-}1]^7[c]^7 & -\mu - k_x[IAP] \end{bmatrix}.$$

Eigenvalues of the Jacobian matrix evaluated at steady state provide a way to determine stability of the given steady state. If real part of the eigenvalue is negative, the steady state is stable in the direction of eigenvector corresponding to the given eigenvalue, and vice versa for eigenvalue with positive real part. If eigenvalue is a complex number, than steady state is a spiral in the dimensions corresponding to the eigenvectors of the given eigenvalue and its complex conjugate.

Figure 3 shows bifurcation diagram for concentration of cytochrome c for modified reduced model. Red line near zero corresponds to the state without apoptosis. The upper part of hyperbola correspond to ongoing apoptosis. In comparison to bifurcation diagram in [23, Figure 11], the limit point of the bifurcation is slightly shifted from roughly $[mit] \approx 0.228$ (corresponding to $\Omega_{Bax} = \Omega_{c_{mito}} \approx 1.14 \cdot 10^{-4}\,\mu\text{Ms}^{-1}$ in [23]) to roughly $[mit] \approx 0.18$. Also, the upper part of hyperbola is approaching the blue unstable line more quickly.

Quite interesting is observation that beginning of the upper part of hyperbola is marked as unstable resulting in three consecutive unstable steady states as concentration of cytochrome c increases. In two dimensional system this is impossible, however, the dynamics of a twelve dimensional system can be very complicated and thus it might be possible for system to has such steady states. So in order to investigate it, we simulated evolution of concentrations while keeping portion of active mitochondria at $[mit] = 0.19$ of compounds starting from two different sets of concentrations: one was near the upper part of hyperbola, the other was near the lower part. We observed that both times concentrations levelled off at the same concentrations that correspond to steady state at the upper part of hyperbola (data not shown).

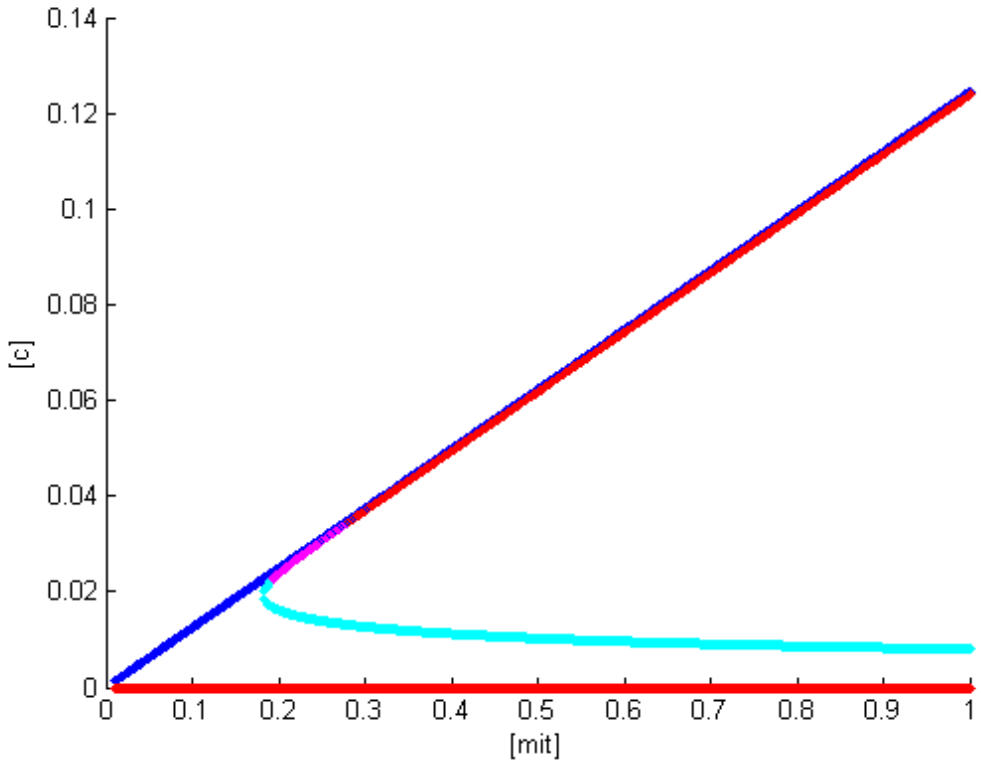

Figure 3: Bifurcation diagram for concentration of cytochrome c (horizontal axis: portion of active mitochondria; vertical axis: concentration of cytochromes c in cytosol; red and magenta for stable nodes and spirals, blue and cyan for unstable nodes and spirals)

Next we take a closer look at line of unstable nodes in Figure 3 (blue line) to determine what is biological meaning of these steady states. However, after drawing bifurcation diagrams for other proteins, we discovered that, in fact, they are not biologically possible since concentrations of Bax are negative (blue line in Figure 4). From mathematical point of view, this could only happen if concentration of Bax_2 is greater than $\Omega_{Bax}/(2\mu)$ (from expression (3.18)). Using mass balance principle we get the following equalities that can be used to find maximal biologically possible concentration of cytochrome c in cytoplasm in steady state:

$$\Omega_{Bax} = \mu[Bax] + 2\mu[Bax_2] \tag{3.23}$$

$$\Omega_{c_{mito}}[mit] = \mu[c_{mito}] + \mu[c] \tag{3.24}$$

We do not need to consider any other equalities as concentrations of all other compounds are non-negative for non-negative concentration of cytochrome c. Equality

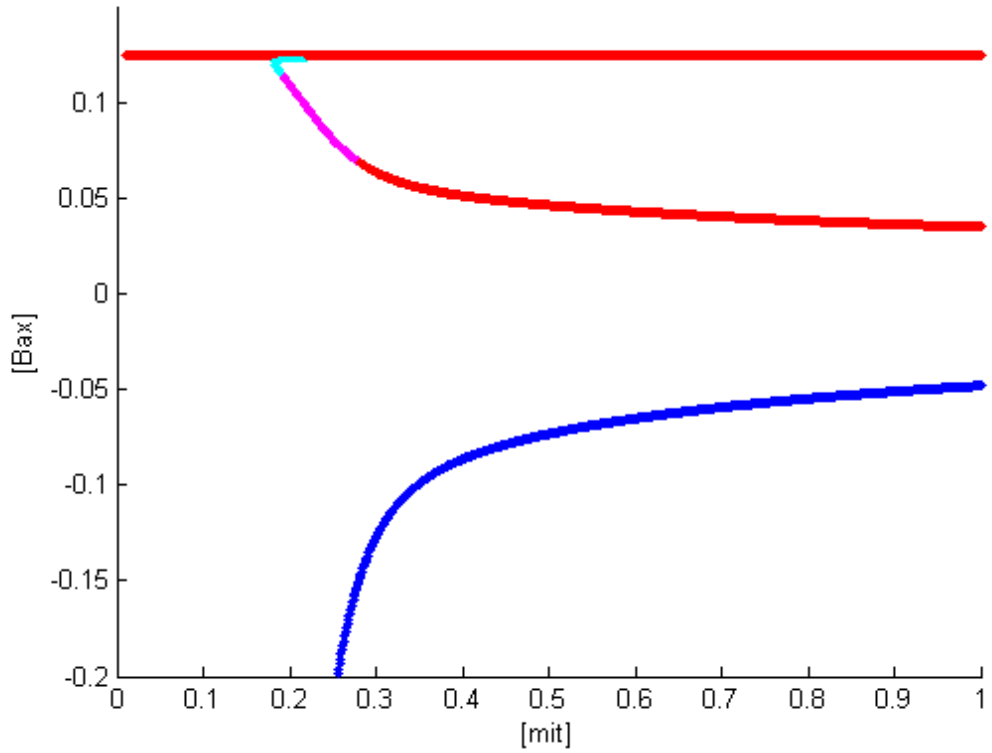

Figure 4: Bifurcation diagram for concentration of Bax protein (horizontal axis: portion of active mitochondria; vertical axis: concentration of Bax; red and magenta for stable nodes and spirals, blue and cyan for unstable nodes and spirals)

(3.23) gives us the upper bound on concentration of Bax_2 in steady state:

$$[Bax_2] \leq \frac{\Omega_{Bax}}{2\mu} \tag{3.25}$$

After substituting expressions for steady state concentrations of Bax_2 and mitochondrial cytochrome c into the above inequality we get the following upper bound for concentration of cytochrome c in cytoplasm in steady state:

$$[c] \leq \frac{\Omega_{c_{mito}}[mit]}{\mu} \cdot \frac{k_3\Omega_{Bax}}{2\mu^2 + k_3\Omega_{Bax}} < \frac{\Omega_{c_{mito}}[mit]}{\mu}. \tag{3.26}$$

4 Mathematical Model of Apoptosis

4.1 Modifications

As in the previous chapter 3, first we propose few modifications to the "full" mathematical model of apoptosis that was proposed in [23, Chapter 4] to address inconsistencies between observed behaviour of the mathematical system and laboratory experiments.

Synthesis of Bax and translocation of tBid to mitochondria

Again we modify synthesis of Bax protein to be independent of portion of active mitochondria as it is predominantly localised in cytosol in healthy cells and is recruited to mitochondria by tBid after the induction of apoptosis [21].

In this model, formation of Bax_2 channels is modelled through two distinct steps:

1. translocation of tBid to mitochondrial outer membrane and
2. the formation itself.

In model proposed in [23, Chapter 4] traslocation of tBid is modelled using one-step uni-molecular kinetic reaction scheme:

$$tBid \xrightarrow{k_{11}} tBid, \tag{4.1}$$

where k_{11} is the corresponding rate. Similarly to reaction (4.2) this leads to accumulation of tBid on mitochondria even thou all mitochondria has already disappeared (data not shown). Therefore we change the kinetic reaction scheme to

$$tBid + mit \xrightarrow{k_{11}} tBid + mit. \tag{4.2}$$

Cooperative formation of an apoptosome complex formation Kinetic reaction schemes for cooperative formation of apoptosome complex used in model proposed in [23, Chapter 4] were adopted from [6] where the reaction order $p = 4$ was used to ensure bistability with regard to initial condition. However, since we could not find biological evidence to support that and our results show the same qualitative behaviour in response to invasion of Trichinella spiralis (Figure 5 from 0 to 2000 s) we decided to change it to fully cooperative formation by setting $p = 7$. This resulted different

qualitative behaviour after mitochondria started reappearing (Figure 5 from 4000 to 12000 s): while for $p = 4$ apoptosis started again (high levels of caspases and AIF), for $p = 7$ it did not.

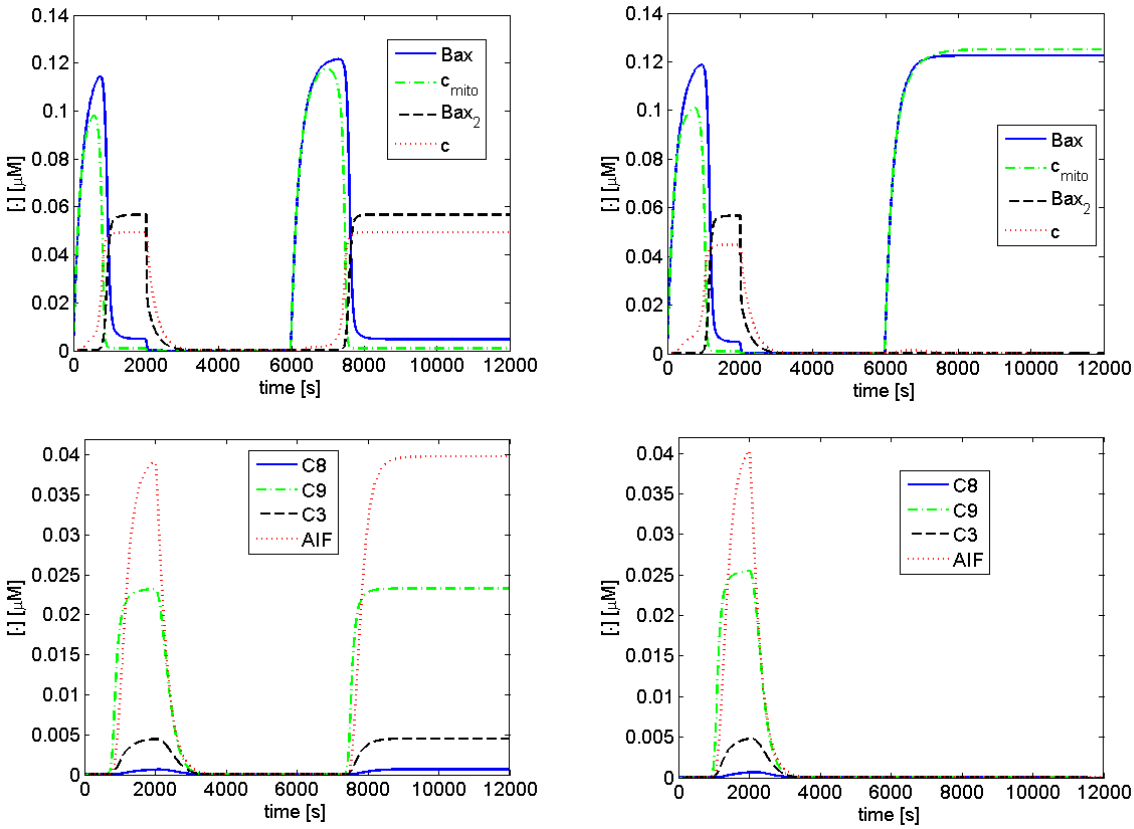

Figure 5: Time evolution of concentrations of selected proteins for reaction order $p = 4$ (left) and $p = 7$ (right) of cooperative formation of apoptosome complex.

Disappearance and appearance of mitochondria Since mitochondria generate most of the cell's supply of ATP that is used as a source of chemical energy for all cellular processes, it is very unlikely that Trichinella spiralis would let all mitochondria disappear as its goal is to transform muscle cell into a nurse cell [12, 43]. Therefore we decided to set a lower bound, mit_{min}, on portion of active mitochondria. In order to do that we need to change how mitochondria are modelled as it needs to be approached smoothly to correspond with behaviour of biological processes.

Mitochondrial dynamics can be divided into two phases: disappearance of old and appearance of the new mitochondria. In the first phase the portion of active mitochondria will be expressed using hyperbolic tangent to smoothly decrease from initial value

of portion of active mitochondria, $[mit]_0 = 1$, to the lower bound mit_{min}:

$$[mit](t) = \frac{1 + mit_{min}}{2} - \frac{1 - mit_{min}}{2} \tanh\left(\frac{t-a}{b}\right), \tag{4.3}$$

where a and b are parameters that regulate time shift and time derivative. We chose their values so that:

- the decrease happens as soon as possible while the difference between $[mit]$ and initial value $[mit]_0$ is less than 10^{-8} during the initial time T_i and
- the absolute value of time derivative of portion of active mitochondria is less than the maximal rate of disappearance of mitochondria r_d.

This translates into the following optimisation problem:

$$\begin{aligned} \underset{a,b>0}{\text{minimise}} \quad & (a, b) \\ \text{subject to} \quad & [mit]_0 - [mit] \leq 10^{-8}, \quad t \leq T_i \\ & |[mit]'(t)| \leq r_d \end{aligned} \tag{4.4}$$

that can be easily solved:

$$b = \frac{[mit]_0 - [mit]}{2r_d}, \quad a = T_i - \frac{b}{2} \ln\left(\frac{10^{-8}}{[mit]_0 - mit_{min} - 10^{-8}}\right). \tag{4.5}$$

Appearance of new mitochondria can be viewed as population growth. One of the most widely used differential equation to describe population growth is logistic equation that for our case is:

$$\dot{[mit]} = r_a \left([mit] - mit_{min}\right)\left(1 - \frac{[mit] - mit_{min}}{mit_{max} - mit_{min}}\right), \tag{4.6}$$

where r_a is the maximal rate of appearance of mitochondria and mit_{max} is the maximal portion of active mitochondria in the cell. So in the second phase we will use analytical solution of the logistic growth equation (4.6) to express portion of active mitochondria:

$$[mit](t) = mit_{min} + \frac{(mit_{max} - mit_{min})([mit]\,(T_a) - mit_{min})e^{r_a t}}{(mit_{max} - mit_{min}) + ([mit]\,(T_a) - mit_{min})\,(e^{r_a t} - 1)}, \tag{4.7}$$

where T_a is the time when new mitochondria start to appear.

Taken together, portion of active mitochondria can be expressed as:

$$[mit](t) = \begin{cases} \frac{1+mit_{min}}{2} - \frac{1-mit_{min}}{2} \tanh\left(\frac{t-a}{b}\right), & t \leq T_i \\ mit_{min} + \frac{(mit_{max}-mit_{min})([mit](T_a)-mit_{min})e^{r_a t}}{(mit_{max}-mit_{min})+([mit](T_a)-mit_{min})(e^{r_a t}-1)}, & t > T_i \end{cases}, \tag{4.8}$$

where a and b are defined in (4.5). The time derivative used to model the effect of mitochondrial dynamics on concentrations stored inside mitochondria is then:

$$dmit(t) = \begin{cases} -\frac{1-mit_{min}}{2b}\left(1-\tanh^2\left(\frac{t-a}{b}\right)\right), & t \leq T_i \\ r_a[mit](t)\left(1-\frac{[mit](t)}{mit_{max}-mit_{min}}\right), & t > T_i \end{cases}. \tag{4.9}$$

4.2 Description of the model

Here we provide summary of the mathematical model proposed in [23, Chapter 4] with our modifications accommodated into it. Graphical representation of the model can be seen in Figure 6. Dynamics of the model is govern by the following biochemical reactions, where k-s are the corresponding kinetic reaction rates as used in the simulations and J-s are the fluxes corresponding to the reactions derived from law of mass action:

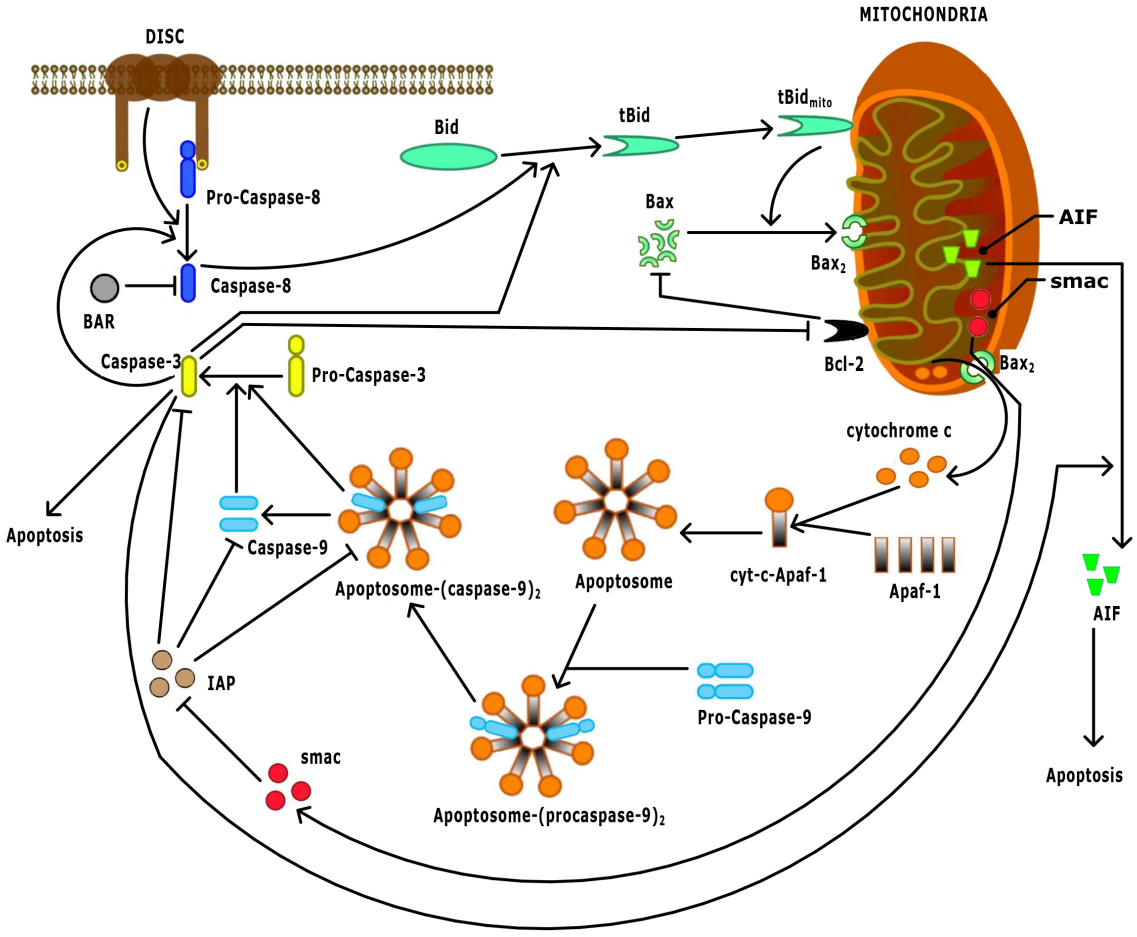

Figure 6: Graphic representation of the model of apoptosis (compare to [23, Fig. 16])

Activation of caspase-8 by DISC

After larva of Trichinella spiralis parasite invade muscle cell it triggers membrane receptors initiating formation of $DISC$ complexes that cleave procaspase-8, $PC8$, to produce active initiator caspase-8, $C8$, [20].

$$DISC + PC8 \xrightarrow{k_D} DISC + C8 \qquad k_D = 10\,\mu\mathrm{M}^{-1}\mathrm{s}^{-1}$$

$$J_D = k_D[DISC][PC8]$$

Inhibition of caspase-8 by BAR

It was proposed that protein termed BAR, bifunctional apoptosis regulator, is able to inhibit active caspase-8 in the similar matter as IAP is able to inhibit active caspases-9 and -3 [15, 36, 46].

$$C8 + BAR \underset{k_B^-}{\overset{k_B^+}{\rightleftharpoons}} C8 \cdot BAR \qquad k_B^+ = 5\,\mu\mathrm{M}^{-1}\mathrm{s}^{-1}$$

$$J_B = k_B^+[C8][BAR] - k_B^-[C8 \cdot BAR] \qquad k_B^- = 0.0035\,\mathrm{s}^{-1}$$

Cleavage of Bid by caspase-8

In the mitochondrial apoptotic pathway upon activation caspase-8 cleaves pro-apoptotic BH3-only protein Bid from the Bcl-2 family to its active form $tBid$ [25, 27].

$$C8 + Bid \underset{k_0^-}{\overset{k_0^+}{\rightleftharpoons}} C8 \cdot Bid \qquad k_0^+ = 10\,\mu\mathrm{M}^{-1}\mathrm{s}^{-1}$$

$$J_0 = k_0^+[C8][Bid] - k_0^-[C8 \cdot Bid] \qquad k_0^- = 0.5\,\mathrm{s}^{-1}$$

$$C8 \cdot Bid \xrightarrow{k_0^f} C8 + tBid \qquad k_0^f = 0.1\,\mathrm{s}^{-1}$$

$$J_0^f = k_0^f[C8 \cdot Bid]$$

Translocation of truncated Bid to mitochondrial outer membrane

Upon cleavage by caspase-8 $tBid$ translocates and inserts itself into the mitochondrial outer membrane where it acts as promoter of apoptotic permeabilisation of mitochondrial outer membrane and release of pro-apoptotic proteins stored in mitochondrial intermembrane space such as cytochrome c and *smac* [18, 28].

$$tBid + mit \xrightarrow{k_{11}} tBid_{mito} + mit \qquad k_{11} = 10\,\mathrm{s}^{-1}$$

$$J_{11} = k_{11}[tBid][mit]$$

Formation of Bax_2 channels in mitochondrial membrane

Mitochondrially localized truncated *Bid* binds with cytosolic *Bax* and induces its homo-oligomerisation and formation of pores in the mitochondrial outer membrane [21, 40, 41].

$$tBid_{mito} + Bax \xrightarrow{k_{12a}} tBid \cdot Bax \qquad k_{12a} = 10\,\mu\mathrm{M}^{-1}\mathrm{s}^{-1}$$

$$J_{12a} = k_{12a}[tBid_{mito}][Bax]$$

$$tBid \cdot Bax + Bax \xrightarrow{k_{12b}} tBid + Bax_2 \qquad k_{12b} = 10\,\mu\mathrm{M}^{-1}\mathrm{s}^{-1}$$

$$J_{12b} = k_{12b}[tBid \cdot Bax][Bax]$$

Release of cytochrome c from mitochondria to cytoplasm

After formation of Bax_2 channels, cytochrome c, *c*, is released from mitochondrial intermembrane space [11, 39, 40].

$$Bax_2 + c_{mito} \xrightarrow{k_{14}} Bax_2 + c \qquad k_{14} = 10\,\mu\mathrm{M}^{-1}\mathrm{s}^{-1}$$

$$J_{14} = k_{14}[Bax_2][c_{mito}]$$

Release of smac from mitochondria to cytoplasm

Similarly to cytochrome c, *smac* is also released through Bax_2 channels [39]

$$Bax_2 + smac_{mito} \xrightarrow{k_{15}} Bax_2 + smac \qquad k_{15} = 10\,\mu\mathrm{M}^{-1}\mathrm{s}^{-1}$$

$$J_{15} = k_{15}[Bax_2][smac_{mito}]$$

Apoptosome complex formation

Once released cytochrome c together with apoptotic protease activating factor 1, *Apaf*-1 forms heptameric complex termed apoptosome, *apop*, [1, 44]. We adopt fully cooperative dynamic of apoptosome complex formation.

$$c + Apaf\text{-}1 \underset{k_{1a}^-}{\overset{k_{1a}^+}{\rightleftharpoons}} c \cdot Apaf\text{-}1 \qquad k_{1a}^+ = 5\,\mu\mathrm{M}^{-1}\mathrm{s}^{-1}$$

$$J_{1a} = k_{1a}^+[c][Apaf\text{-}1] - k_{1a}^-[c \cdot Apaf\text{-}1] \qquad k_{1a}^- = 0.5\,\mathrm{s}^{-1}$$

$$7\,(c \cdot Apaf\text{-}1) \underset{k_{1b}^-}{\overset{k_{1b}^+}{\rightleftharpoons}} apop \qquad k_{1b}^+ = 5 \cdot 104\,\mu\mathrm{M}^{-3}\mathrm{s}^{-1}$$

$$J_{1b} = k_{1b}^+[c \cdot Apaf\text{-}1]^4 - k_{1b}^-[apop] \qquad k_{1b}^- = 0.5\,\mathrm{s}^{-1}$$

Activation of caspase-9 by apoptosome

In order for apoptosome to activate initiator caspase-9, $C9$, two procaspase-9, $PC9$, molecules must bind to the apoptosome [17,47]. Two step detachment of active caspase-9 molecules is adopted.

$$apop + PC9 \underset{k_{2a}^-}{\overset{k_{2a}^+}{\rightleftharpoons}} apop \cdot PC9 \qquad k_{2a}^+ = 10\,\mu\mathrm{M}^{-1}\mathrm{s}^{-1}$$

$$J_{2a} = k_{2a}^+[apop][PC9] - k_{2a}^-[apop \cdot PC9] \qquad k_{2a}^- = 0.5\,\mathrm{s}^{-1}$$

$$apop \cdot PC9 + PC9 \underset{k_{2b}^-}{\overset{k_{2b}^+}{\rightleftharpoons}} apop \cdot PC9 \qquad k_{2b}^+ = 10\,\mu\mathrm{M}^{-1}\mathrm{s}^{-1}$$

$$J_{2b} = k_{2b}^+[apop \cdot PC9][PC9] - k_{2b}^-[apop \cdot (PC9)_2] \qquad k_{2b}^- = 0.5\,\mathrm{s}^{-1}$$

$$apop \cdot (PC9)_2 \xrightarrow{k_3} apop \cdot (C9)_2 \qquad k_3 = 0.1\,\mathrm{s}^{-1}$$

$$J_3 = k_3[apop \cdot (PC9)_2]$$

$$apop \cdot (C9)_2 \underset{k_{4a}^-}{\overset{k_{4a}^+}{\rightleftharpoons}} apop \cdot C9 + C9 \qquad k_{4a}^+ = 5\,\mathrm{s}^{-1}$$

$$J_{4a} = k_{4a}^+[apop \cdot (C9)_2] - k_{4a}^-[apop \cdot C9][C9] \qquad k_{4a}^- = 0.5\,\mu\mathrm{M}^{-1}\mathrm{s}^{-1}$$

$$apop \cdot C9 \underset{k_{4b}^-}{\overset{k_{4b}^+}{\rightleftharpoons}} apop + C9 \qquad k_{4b}^+ = 5\,\mathrm{s}^{-1}$$

$$J_{4b} = k_{4b}^+[apop \cdot C9] - k_{4b}^-[apop][C9] \qquad k_{4b}^- = 0.5\,\mu\mathrm{M}^{-1}\mathrm{s}^{-1}$$

Activation of caspase-3 by caspase-9

Active caspase-9 has the ability to cleave procaspase-3 to yield active executioner caspase-3 molecule [17].

$$C9 + PC3 \underset{k_{6a}^-}{\overset{k_{6a}^+}{\rightleftharpoons}} C9 \cdot PC3 \qquad k_{6a}^+ = 10\,\mu\mathrm{M}^{-1}\mathrm{s}^{-1}$$

$$J_{6a} = k_{6a}^+[C9][PC3] - k_{6a}^-[C9 \cdot PC3] \qquad k_{6a}^- = 0.5\,\mathrm{s}^{-1}$$

$$C9 \cdot PC3 \xrightarrow{k_{6a}^f} C9 + C3 \qquad k_{6a}^f = 0.001\,\mathrm{s}^{-1}$$

$$J_{6a}^f = k_{6a}^f[C9 \cdot PC3]$$

Another mechanism of activation of caspase-3

Complex consisting of apoptosome and two active caspase-9 molecules can activate caspase-3 by cleaving procaspase-3 [30, 31]

$$apop \cdot (C9)_2 + PC3 \underset{k_{6b}^-}{\overset{k_{6b}^+}{\rightleftharpoons}} apop \cdot (C9)_2 \cdot PC3 \qquad k_{6b}^+ = 10\,\mu\mathrm{M}^{-1}\mathrm{s}^{-1}$$

$$J_{6b} = k_{6b}^+[apop \cdot (C9)_2][PC3] - k_{6b}^-[apop \cdot (C9)_2 \cdot PC3] \qquad k_{6b}^- = 0.5\,\mathrm{s}^{-1}$$

$$apop \cdot (C9)_2 \cdot PC3 \xrightarrow{k_{6b}^f} apop \cdot (C9)_2 + C3 \qquad k_{6b}^f = 0.1\,\mathrm{s}^{-1}$$

$$J_{6b}^f = k_{6b}^f[apop \cdot (C9)_2 \cdot PC3]$$

Loop activation of caspase-8 by caspase-3

Active caspase-3 is able to activate initiator caspase-8 [15, 17], serving as a positive feedback loop to amplify initial apoptotic signal.

$$C3 + PC8 \underset{k_x^-}{\overset{k_x^+}{\rightleftharpoons}} C3 \cdot PC8 \qquad k_x^+ = 10\,\mu\mathrm{M}^{-1}\mathrm{s}^{-1}$$

$$J_x = k_x^+[C3][PC8] - k_x^-[C3 \cdot PC8] \qquad k_x^- = 0.5\,\mathrm{s}^{-1}$$

$$C3 \cdot PC8 \xrightarrow{k_x^f} C3 + C8 \qquad k_x^f = 0.001\,\mathrm{s}^{-1}$$

$$J_x^f = k_x^f[C3 \cdot PC8]$$

Inhibition of caspase-9 by IAP

Inhibitor of apoptosis, IAP, has the ability to inhibit active caspase-9 in all its forms through reversible binding [24, 32, 34].

$$C9 + IAP \underset{k_{5a}^-}{\overset{k_{5a}^+}{\rightleftharpoons}} C9 \cdot IAP \qquad k_{5a}^+ = 5\,\mu\mathrm{M}^{-1}\mathrm{s}^{-1}$$

$$J_{5a} = k_{5a}^+[C9][IAP] - k_{5a}^-[C9 \cdot IAP] \qquad k_{5a}^- = 0.0035\,\mathrm{s}^{-1}$$

$$apop \cdot C9 + IAP \underset{k_{5b}^-}{\overset{k_{5b}^+}{\rightleftharpoons}} apop \cdot C9 \cdot IAP \qquad k_{5b}^+ = 5\,\mu\mathrm{M}^{-1}\mathrm{s}^{-1}$$

$$J_{5b} = k_{5b}^+[apop \cdot C9][IAP] - k_{5b}^-[apop \cdot C9 \cdot IAP] \qquad k_{5b}^- = 0.0035\,\mathrm{s}^{-1}$$

$$apop \cdot (C9)_2 + IAP \underset{k_{5c}^-}{\overset{k_{5c}^+}{\rightleftharpoons}} apop \cdot (C9)_2 \cdot IAP \qquad k_{5c}^+ = 5\,\mu\mathrm{M}^{-1}\mathrm{s}^{-1}$$

$$J_{5c} = k_{5c}^+[apop \cdot (C9)_2][IAP] - k_{5c}^-[apop \cdot (C9)_2 \cdot IAP] \qquad k_{5c}^- = 0.0035\,\mathrm{s}^{-1}$$

Inhibition of caspase-3 by IAP

IAP is able to inhibit activity of active caspase-3 through the same mechanism of reversible binding [17,24,32]. In [24] was inhibitory ability of IAP identified as possible cause for the bistable apoptotic behaviour.

$$C3 + IAP \underset{k_7^-}{\overset{k_7^+}{\rightleftharpoons}} C3 \cdot IAP \qquad k_7^+ = 5\,\mu\mathrm{M}^{-1}\mathrm{s}^{-1}$$

$$J_7 = k_7^+[C3][IAP] - k_7^-[C3 \cdot IAP] \qquad k_7^- = 0.0035\,\mathrm{s}^{-1}$$

Inhibition of IAP by smac

Mitochondrial pro-apoptotic protein $smac/DIABLO$ promotes apoptosis by sequestering inhibitors of apoptosis [15,32].

$$IAP + smac \underset{k_{SM}^-}{\overset{k_{SM}^+}{\rightleftharpoons}} IAP \cdot smac \qquad k_{SM}^+ = 5\,\mu\mathrm{M}^{-1}\mathrm{s}^{-1}$$

$$J_{SM} = k_{SM}^+[IAP][smac] - k_{SM}^-[IAP \cdot smac] \qquad k_{SM}^- = 0.0035\,\mathrm{s}^{-1}$$

Loop cleavage of Bid by caspase-3

In addition to caspase-8, active caspase-3 has also the ability to truncate Bid to $tBid$ [27,35]. Serving as a second positive feedback loop of the model.

$$C3 + Bid \underset{k_8^-}{\overset{k_8^+}{\rightleftharpoons}} C3 \cdot Bid \qquad k_8^+ = 10\,\mu\mathrm{M}^{-1}\mathrm{s}^{-1}$$

$$J_8 = k_8^+[C3][Bid] - k_8^-[C3 \cdot Bid] \qquad k_8^- = 0.5\,\mathrm{s}^{-1}$$

$$C3 \cdot Bid \xrightarrow{k_8^f} C3 + tBid \qquad k_8^f = 0.1\,\mathrm{s}^{-1}$$

$$J_8^f = k_8^f[C3 \cdot Bid]$$

Inhibition of Bax by Bcl-2

Since Bax is essential effector of the mitochondria-mediated apoptotic pathway, its pro-apoptotic acitivity tighly kept in check by anti-apoptotic protein Bcl-2 [3] that binds to cytosolic Bax thus slowing the channel formation for cytochrome c and $smac$ release.

$$Bax + Bcl\text{-}2 \xrightarrow{k_{13}} (Bax \cdot Bcl\text{-}2)_{inactive} \qquad k_{13} = 10\,\mu\mathrm{M}^{-1}\mathrm{s}^{-1}$$

$$J_{13} = k_{13}[Bax][Bcl\text{-}2]$$

Cleavage (inactivation) of Bcl-2 by caspase-3

The cleavage of anti-apoptotic protein *Bcl*-2 by active caspase-3 [22] serves as the third and last positive feedback loop.

$$C3 + Bcl\text{-}2 \underset{k_9^-}{\overset{k_9^+}{\rightleftharpoons}} C3 \cdot Bcl\text{-}2 \qquad k_9^+ = 10\,\mu\mathrm{M}^{-1}\mathrm{s}^{-1}$$

$$J_9 = k_9^+[C3][Bcl\text{-}2] - k_9^-[C3 \cdot Bcl\text{-}2] \qquad k_9^- = 0.5\,\mathrm{s}^{-1}$$

$$C3 \cdot Bcl\text{-}2 \xrightarrow{k_9^f} C3 + Bcl\text{-}2_{cleaved} \qquad k_9^f = 0.1\,\mathrm{s}^{-1}$$

$$J_9^f = k_9^f[C3 \cdot Bcl\text{-}2]$$

Release of AIF from mitochondria to cytoplasm

Apoptosis-inducing factor, AIF, plays a significant role in nuclear changes during apoptosis [37]. It is normally localized in the mitochondrial intermembrane space where it is tethered to the mitochondrial inner membrane. Consequently, its release from mitochondria requires proteolytic cleavage by caspases [4]. According to [19] AIF is released from mitochondria by caspase-2, which is activated by caspase-3 [7]. Here the activation of caspase-2 is omitted.

$$C3 + AIF_{mito} \xrightarrow{k_{20}} C3 + AIF \qquad k_{20} = 1\,\mu\mathrm{M}^{-1}\mathrm{s}^{-1}$$

$$J_{20} = k_{20}[C3][AIF_{mito}]$$

Synthesis and degradation of molecules

The initial concentrations of all compounds are zero except for $DISC$ and procaspase-8 with initial values of 10^{-4}, that serve as an initial apoptotic signal triggered by invasion of Trichinalla spiralis. portion of active mitochondria is set to 1. All primary forms of proteins, that is $PC8$, BAR, Bid, Bax, c_{mito}, $smac_{mito}$, $Apaf\text{-}1$, $PC9$, $PC3$, IAP, $Bcl\text{-}2$ and AIF_{mito}, are synthesized according to the following reactions with corresponding synthesis rates Ω.

$$\varnothing \xrightarrow{\Omega_{PC8}} PC8 \qquad \Omega_{PC8} = 6 \cdot 10^{-4}\,\mu\mathrm{Ms}^{-1}$$

$$\varnothing \xrightarrow{\Omega_{BAR}} BAR \qquad \Omega_{BAR} = 3 \cdot 10^{-5}\,\mu\mathrm{Ms}^{-1}$$

$$\varnothing \xrightarrow{\Omega_{Bid}} Bid \qquad \Omega_{Bid} = 6 \cdot 10^{-5}\,\mu\mathrm{Ms}^{-1}$$

$$\varnothing \xrightarrow{\Omega_{Bax}} Bax \qquad \Omega_{Bax} = 5 \cdot 10^{-4}\,\mu\mathrm{Ms}^{-1}$$

$$mit \xrightarrow{\Omega_{c_{mito}}} c_{mito} \qquad \Omega_{c_{mito}} = 5 \cdot 10^{-4}\,\mu\mathrm{Ms}^{-1}$$

$$mit \xrightarrow{\Omega_{smac_{mito}}} smac_{mito} \qquad \Omega_{smac_{mito}} = 5 \cdot 10^{-4}\,\mu\mathrm{Ms}^{-1}$$

$$\varnothing \xrightarrow{\Omega_{Apaf\text{-}1}} Apaf\text{-}1 \qquad \Omega_{Apaf\text{-}1} = 6 \cdot 10^{-4}\,\mu\mathrm{Ms}^{-1}$$

$$\varnothing \xrightarrow{\Omega_{PC9}} PC9 \qquad \Omega_{PC9} = 6 \cdot 10^{-4}\,\mu\mathrm{Ms}^{-1}$$

$$\varnothing \xrightarrow{\Omega_{PC3}} PC3 \qquad \Omega_{PC3} = 6 \cdot 10^{-4}\,\mu\mathrm{Ms}^{-1}$$

$$\varnothing \xrightarrow{\Omega_{IAP}} IAP \qquad \Omega_{IAP} = 3 \cdot 10^{-5}\,\mu\mathrm{Ms}^{-1}$$

$$mit \xrightarrow{\Omega_{Bcl\text{-}2}} Bcl\text{-}2 \qquad \Omega_{Bcl\text{-}2} = 10^{-5}\,\mu\mathrm{Ms}^{-1}$$

$$mit \xrightarrow{\Omega_{AIF_{mito}}} AIF_{mito} \qquad \Omega_{AIF_{mito}} = 3 \cdot 10^{-4}\,\mu\mathrm{Ms}^{-1}$$

A first order degradation kinetics with a uniform rate constant of $\mu = 0.004$ is adopted for all compounds except for *mit* that does not degrade and $DISC$ that after serving as initial apoptotic signal quickly degrades at constant rate $\mu_{DISC} = 100\mu$.

The above biochemical reactions translate into the following system of ordinary differential equations:

$$\dot{[DISC]} = -100\mu[DISC] \tag{4.10}$$

$$\dot{[PC8]} = \Omega_{PC8} - \mu[PC8] - J_D - J_x \tag{4.11}$$

$$\dot{[C8]} = -\mu[C8] + J_D + J_x^f - J_B - J_0 + J_0^f \tag{4.12}$$

$$\dot{[BAR]} = \Omega_{BAR} - \mu[BAR] - J_B \tag{4.13}$$

$$\dot{[C8 \cdot BAR]} = -\mu[C8 \cdot BAR] + J_B \tag{4.14}$$

$$\dot{[Bid]} = \Omega_{Bid} - \mu[Bid] - J_0 - J_8 \tag{4.15}$$

$$\dot{[C8 \cdot Bid]} = -\mu[C8 \cdot Bid] + J_0 - J_0^f \tag{4.16}$$

$$\dot{[tBid]} = -\mu[tBid] + J_0^f + J_8^f - J_{11} + J_{12b} \tag{4.17}$$

$$\dot{[tBid_{mito}]} = -\mu[tBid_{mito}] + J_{11} - J_{12a} + dmit[tBid_{mito}] \tag{4.18}$$

$$\dot{[Bax]} = \Omega_{Bax} - \mu[Bax] - J_{12a} - J_{12b} - J_{13} \tag{4.19}$$

$$\dot{[tBid \cdot Bax]} = -\mu[tBid \cdot Bax] + J_{12a} - J_{12b} + dmit[tBid \cdot Bax] \tag{4.20}$$

$$\dot{[Bax_2]} = -\mu[Bax_2] + J_{12b} + dmit[Bax_2] \tag{4.21}$$

$$\dot{[c_{mito}]} = \Omega_{c_{mito}}[mit] - \mu[c_{mito}] - J_{14} + dmit[c_{mito}] \tag{4.22}$$

$$\dot{[c]} = -\mu[c] + J_{14} - J_{1a} \tag{4.23}$$

$$\dot{[smac_{mito}]} = \Omega_{smac_{mito}}[mit] - \mu[smac_{mito}] - J_{15} + dmit[smac_{mito}] \tag{4.24}$$

$$\dot{[smac]} = -\mu[smac] + J_{15} - J_{SM} \tag{4.25}$$

$$\dot{[Apaf\text{-}1]} = \Omega_{Apaf\text{-}1} - \mu[Apaf\text{-}1] - J_{1a} \tag{4.26}$$

$$\dot{[c \cdot Apaf\text{-}1]} = -\mu[c \cdot Apaf\text{-}1] + J_{1a} - 7J_{1b} \tag{4.27}$$

$$\dot{[apop]} = -\mu[apop] + J_{1b} - J_{2a} + J_{4b} \tag{4.28}$$

$$\dot{[PC9]} = \Omega_{PC9} - \mu[PC9] - J_{2a} - J_{2b} \tag{4.29}$$

$$\dot{[apop \cdot PC9]} = -\mu[apop \cdot PC9] + J_{2a} - J_{2b} \tag{4.30}$$

$$\dot{[apop \cdot (PC9)_2]} = -\mu[apop \cdot (PC9)_2] + J_{2b} - J_3 \tag{4.31}$$

$$\dot{[apop \cdot (C9)_2]} = -\mu[apop \cdot (C9)_2] + J_3 - J_{4a} - J_{5c} - J_{6b} + J_{6b}^f \tag{4.32}$$

$$\dot{[apop \cdot C9]} = -\mu[apop \cdot C9] + J_{4a} - J_{4b} - J_{5b} \tag{4.33}$$

$$\dot{[C9]} = -\mu[C9] + J_{4a} + J_{4b} - J_{5a} - J_{6a} + J_{6a}^f \tag{4.34}$$

$$\dot{[PC3]} = \Omega_{PC3} - \mu[PC3] - J_{6a} - J_{6b} \tag{4.35}$$

$$\dot{[C9 \cdot PC3]} = -\mu[C9 \cdot PC3] + J_{6a} - J_{6a}^f \tag{4.36}$$

$$\dot{[apop \cdot (C9)_2 \cdot PC3]} = -\mu[apop \cdot (C9)_2 \cdot PC3]] + J_{6b} - J_{6b}^f \tag{4.37}$$

$$\dot{[C3]} = -\mu[C3] + J_{6a}^f + J_{6b}^f - J_7 - J_x + J_x^f - J_8 + J_8^f - J_9 + J_9^f \tag{4.38}$$

$$\dot{[C3 \cdot PC8]} = -\mu[C3 \cdot PC8] + J_x - J_x^f \tag{4.39}$$

$$\dot{[IAP]} = \Omega_{IAP} - \mu[IAP] - J_{5a} - J_{5b} - J_{5c} - J_7 - J_{SM} \tag{4.40}$$

$$\dot{[C9 \cdot IAP]} = -\mu[C9 \cdot IAP] + J_{5a} \tag{4.41}$$

$$\dot{[apop \cdot C9 \cdot IAP]} = -\mu[apop \cdot C9 \cdot IAP] + J_{5b} \tag{4.42}$$

$$\dot{[apop \cdot (C9)_2 \cdot IAP]} = -\mu[apop \cdot (C9)_2 \cdot IAP] + J_{5c} \tag{4.43}$$

$$\dot{[C3 \cdot IAP]} = -\mu[C3 \cdot IAP] + J_7 \tag{4.44}$$

$$\dot{[IAP \cdot smac]} = -\mu[IAP \cdot smac] + J_{SM} \tag{4.45}$$

$$\dot{[C3 \cdot Bid]} = -\mu[C3 \cdot Bid] + J_8 - J_8^f \tag{4.46}$$

$$\dot{[Bcl\text{-}2]} = \Omega_{Bcl\text{-}2}[mit] - \mu[Bcl\text{-}2] - J_{13} - J_9 + dmit[Bcl\text{-}2] \tag{4.47}$$

$$\dot{[Bax \cdot Bcl\text{-}2]} = -\mu[Bax \cdot Bcl\text{-}2] + J_{13} + dmit[Bax \cdot Bcl\text{-}2] \tag{4.48}$$

$$\dot{[C3 \cdot Bcl\text{-}2]} = -\mu[C3 \cdot Bcl\text{-}2] + J_9 - J_9^f + dmit[C3 \cdot Bcl\text{-}2] \tag{4.49}$$

$$\dot{[Bcl\text{-}2_{cleaved}]} = -\mu[Bcl\text{-}2_{cleaved}] + J_9^f + dmit[Bcl\text{-}2_{cleaved}] \tag{4.50}$$

$$[\dot{AIF}_{mito}] = \Omega_{AIF_{mito}}[mit] - \mu[AIF_{mito}] - J_{20} + dmit[AIF_{mito}] \tag{4.51}$$

$$[\dot{AIF}] = -\mu[AIF] + J_{20} \tag{4.52}$$

where Ω_X is the production rate of the molecule X, μ is decomposition rate and is the same for all substances, k-s are the kinetic reaction rates given above with the related reactions and J-s are the fluxes defined above with the related biochemical reactions derived according to law of mass action and $dmit$ is the time derivative of the portion of active mitochondria defined by (4.9).

4.3 Sensitivity analysis

First we need to determine whether larva of Trichinella spiralis parasite can indeed control apoptosis in host muscle cells as was proposed in [5], especially whether it can be stopped by deactivating mitochondria. So we set maximal rate of disapperance of mitochondria to $r_d = 0.1$ and initial time period to $T_i = 2000\,\mathrm{s}$ and systematically varied minimal portion of active mitochondria mit_{min}. Results are shown in Figure 7. From this we conclude that in order to fully stop the ongoing apoptosis, Trichinella

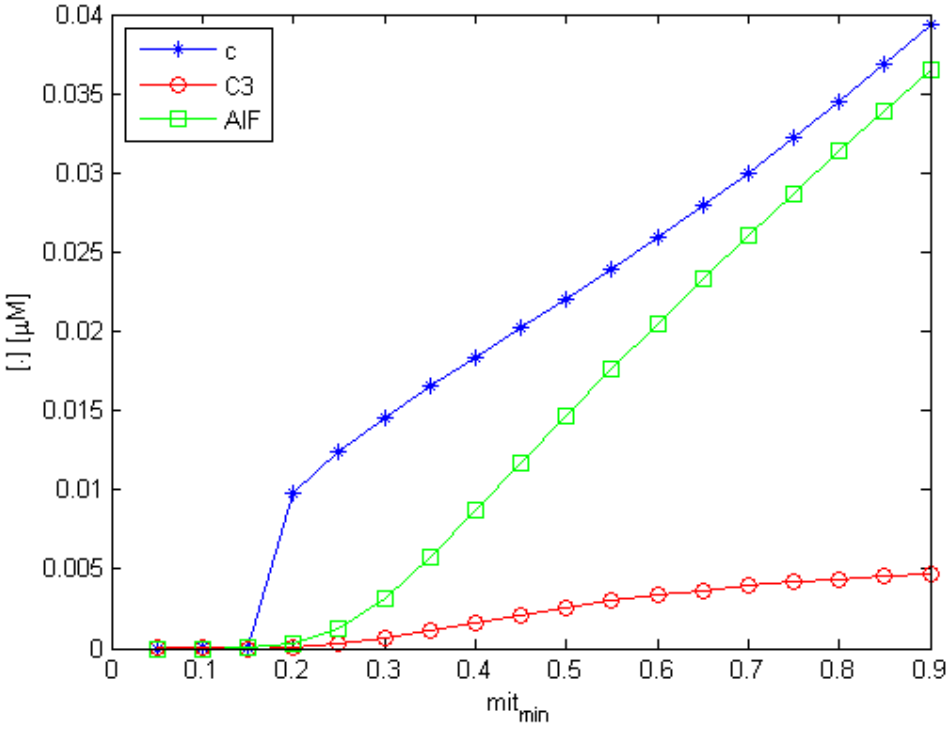

Figure 7: Apoptotical activity with respect to minimal portion of active mitochondria.

needs to decrease portion of active mitochondria below the value of 0.2, as concentrations of cytochrome c, caspase-3 and AIF are negligible. Also graph of concentration of cytochrome s indicates switch like behaviour that is typical for systems that exhibit bistable behaviour.

Next we investigated effects of parameters that represent effect of Trichinella spiralis, i.e. the maximal rate of disappearance of mitochondria r_d, the length of time interval during which disappearance of mitochondria occurs T_d, the maximal rate of appearance of new mitochondria r_a and the maximal portion of active mitochondria mit_{max}. Default values of parameters that were used in simulations are $r_d = 0.1$, $T_d = 3500$, $r_a = 0.1$ and mit_{max}. First we varied (inside a reasonable range of values) only single parameter at a time while keeping other fixed at their default levels and found out that, except for the maximal rate of disappearance of mitochondria, each parameter has a range of values that correspond to the re-start of apoptosis after new mitochondria appear and a range where apoptosis do not start again (data not shown), suggesting that Trichinella must carefully balance their effects.

To determine which parameter is has the strongest influence whether apoptosis would start again after new mitochondria start to appear, we systematically varied two parameters at a time (Figure 8). From the results we conclude that the length of time interval during which disappearance of mitochondria occurs T_d plays the crucial role in accommodation of Trichinella spiralis in muslce cells, as there was no significant apoptotic activity when new mitochondria started appearing 4500 s after beginning of disappearance of old mitochondria.

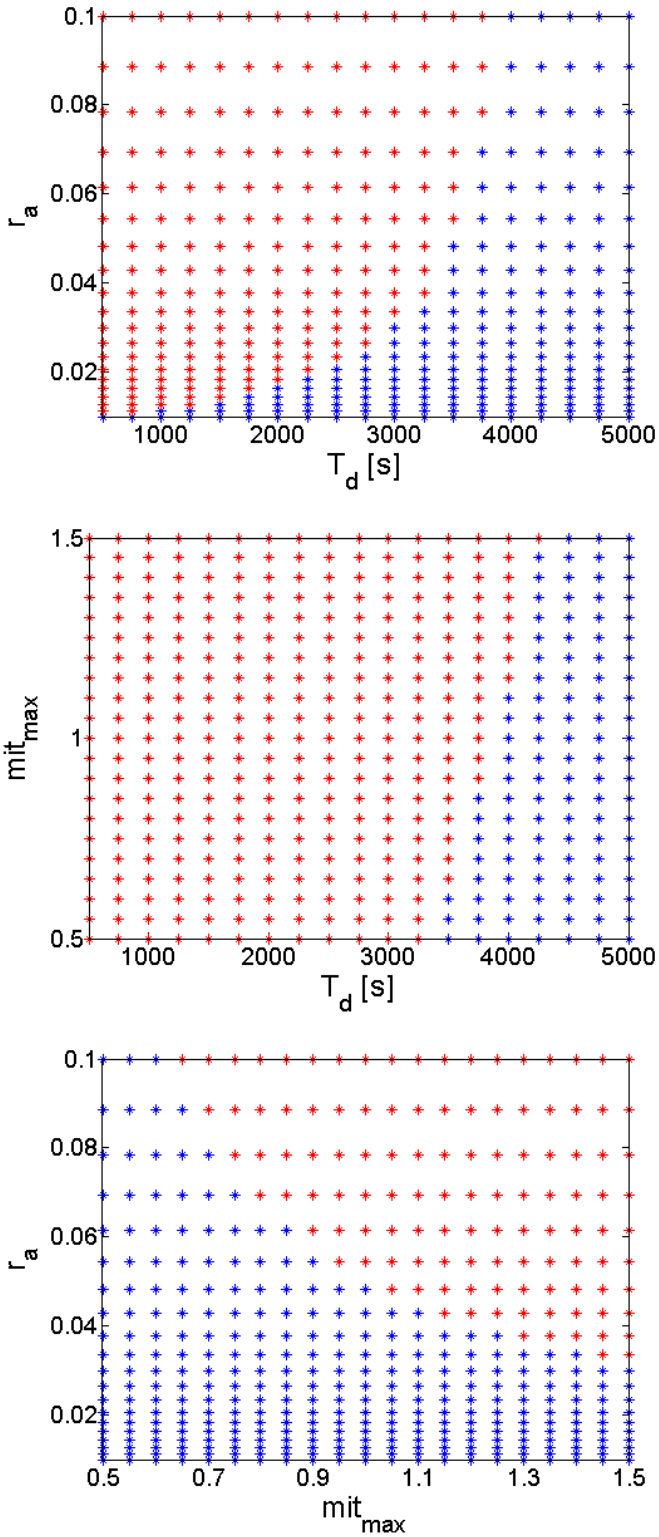

Figure 8: Interactions between chosen parameters that represent influence of Trichinella spiralis in proposed model. Blue color represents no apoptotic activity after new mitochondria appeared, red represents re-start of apoptosis.

5 Expanded Model of Apoptosis

5.1 Modifications and expansion

DNA fragmentation during apoptosis

We expand model from chapter 4 to incorporate process of DNA fragmentation as it is a part of apoptotis in cells. DNA fragmentation is usually a two-step process during which DNA is first cleaved into 50- to 300-kb fragments (high molecular weight DNA fragmentation) and then degraded into smaller fragments of oligonucleosomal size (low molecular weight DNA fragmentation).

Apoptosis inducing factor, AIF, has been demonstrated to play a role in high molecular weight DNA fragmentation [37]. However, AIF lacks nuclease activity activity, suggesting that it promotes DNA fragmentation through activation of yet unidentified nuclease [37] that cleaves DNA. Translocation of AIF and activation of $DNase$ is modelled using law of mass action, while DNA fragmentation is modelled phenomenologically by the following expression:

$$J_{23} = k_{23} \cdot F([DNA]; \alpha_{23}, \beta_{23}) \cdot [DNase_{active}], \tag{5.1}$$

where k_{23} is the maximal rate at which active $DNase$ is able to cleave DNA and function F is a cumulative distribution function of Beta distribution with shape parameters α_{23} and β_{23}:

$$F([DNA]; \alpha_{23}, \beta_{23}) = \frac{\int_0^{[DNA]} x^{\alpha_{23}-1}(1-x)^{\beta_{23}}\mathrm{d}x}{\int_0^1 x^{\alpha_{23}-1}(1-x)^{\beta_{23}}\mathrm{d}x} \tag{5.2}$$

We use cumulative distribution function of the Beta distribution as it has good properties:

- it goes from zero to one on interval $[0, 1]$ (range of values of variable $[DNA]$) and
- can be easily skewed towards 1 to represent inability of $DNase$ to cleave DNA into small fragments.

Caspase-activated DNase, CAD, is responsible for low molecular weight DNA fragmentation [26]. In proliferating cells CAD is kept inactive in cytoplasm associated to the inhibitor of CAD, $ICAD$, [16]. $ICAD$ is expressed in two forms long, $ICAD$-L, and short, $ICAD$-S, however, in our model we will consider both forms as together.

Apart from its inhibitory function, $ICAD$ acts as a chaperone for correct folding of CAD during synthesis, after which it remains associated with CAD.

In order to activate CAD, $ICAD$ needs to be cleaved by caspase-3 at caspase recognition sites Asp^{117} and Asp^{224} [26, 42]. In [45] it was shown that cleavage of $ICAD$ at site Asp^{117} is sufficient for activation of CAD. However, since there is no evidence of preference of caspase-3 to cleave one site or the other, in our model half the time cleavage of compound $CAD \cdot ICAD$ by caspase-3 leads to active CAD (this corresponds to cleavage at site Asp^{117}) and the other half it leads to compound $CAD \cdot ICAD_{Asp^{224}}$ (this corresponds to cleavage at site Asp^{224}).

Active CAD forms dimer CAD_2 with a scissor like shape [42]. Apart from inhibiting active CAD by binding, $ICAD$ has the ability to disassemble the CAD_2 scissors [42]. Low molecular weight DNA fragmentation by CAD_2 dimer is modelled phenomenologically by the following expression:

$$J_{29} = k_{29} \cdot \hat{f}([DNA]; \alpha_{29}, \beta_{29}) \cdot [CAD_{2,nuc}], \tag{5.3}$$

where k_{29} is the maximal rate at which CAD_2 dimer is able to fragment DNA and function $\hat{f}$ is the probability density function of Beta distribution with shape parameters α_{29} and β_{29} normalised so that the maximum is one:

$$\hat{f}(x; \alpha, \beta) = \frac{x^{\alpha-1}(1-x)^{\beta-1}}{b^{\alpha-1}(1-b)^{\beta-1}}, \tag{5.4}$$

where $x = \frac{\alpha-1}{\alpha+\beta-2}$ is the mode of probability density function of Beta distribution. We use probability density function of Beta distribution for similar reasons as cumulative distribution function of Beta distribution for cleavage of DNA by active $DNase$

There exists mechanisms that can repair even fragmented DNA. But, since they are regulated by proteins that are synthesised from DNA, we will model it phenomenologically as a self-repair ability of the DNA by the following expression:

$$J_{30} = k_{30} \cdot \hat{f}([DNA]; \alpha_{30}, \beta_{30}), \tag{5.5}$$

where k_{30} is the maximal rate at which DNA can repair itself and function $\hat{f}$ is the probability density function of Beta distribution with shape parameters α_{30} and β_{30} normalised so that the maximum is one and is defined by the (5.4).

Mitochondrial dynamics

Models analysed in chapters 3 and 4 were based on the assumption that Trichinella spiralis is the reason behind observations of swelling and disappearance of old mitochondria and appearance of new smaller mitochondria near nucleus in muscle cells infected with larva of Trichinella spiralis made in [43]. However, many studies (e.g. [10,33]) show that mitochondrial fragmentation from long filamentous tubules covering the mojority of the cell into numerous small punctate particles and subsequent clustering around nucleus is naturally occurring phenomenon during apoptosis.

Although mitochondrial fragmentation usually accompanies cytochrome c is released from mitochondrial intermembrane space, the separation of these two events during Bax-induced apoptosis [33] demonstrated that they are not inter-dependent steps. Also many groups have observed dramatically fragmented mitochondria in healthy cells [9, 33, 38] suggesting that mitochondrial fragmentation alone is not sufficient to induce apoptosis. Therefore we assume that rather than to facilitate disappearance of mitochondria itself, Trichinella spiralis takes advantage of the naturally occurring fragmentation to accommodate itself in skeletal muscle cells.

In order to accommodate this view into model, we need to make few modifications. Natural modification would be for variable $[mit]$ to model the size or degree of fragmentation of mitochondria. However, since the regulation of mechanism of mitochondrial fragmentation during apoptosis is still unclear, we will model mitochondrial activity rather than actual mitochondria. We assume that formation of Bax_2 pores in mitochondrial outer membrane has direct effect on mitochondrial activity as a consequence of disruption of membrane integrity. The negative effect of Bax_2 channels on mitochondrial activity will be model by the following reaction scheme:

$$mit + Bax_2 \xrightarrow{k_{31}} mit + mit_{inactive} + Bax_2 \qquad k_{31} = 0.001\,\mathrm{s}^{-1}$$

$$J_{31} = k_{31}\frac{[Bax_2]}{M_{Bax_2}}[mit] \qquad M_{Bax_2} = 0.052\,\mu\mathrm{M}$$

where M_{Bax_2} is the maximal concentration of Bax_2 channels as there is only a finite number of sites on mitochondrial outer membrane where pores can form and was obtained by simulating the model without the effect of pores on mitochondrial activity.

We also assume that mitochondria are able to repair the damage caused by Bax_2 pores:

$$mit + mit_{inactive} \xrightarrow{k_{32}} mit \qquad k_{32} = 0.01\,\mathrm{s}^{-1}$$

$$J_{32} = k_{32}\left(1 - \frac{[Bax_2]}{M_{Bax_2}}\right)(1 - [mit]) \qquad M_{Bax_2} = 0.052\,\mu\mathrm{M}$$

Effect of Trichinella spiralis in expanded model

Apoptosis in skeletal muscle is unique because skeletal muscle is myonucleated and thus, the decay of one myonucleus by apoptosis will not produce "wholesale" muscle cell death [2]. Therefore we assume that during invasion into muscle cell Trichinella spiralis on purpose triggers and apoptosis localised to one myonuclear domain and then hijacks the muscle cell repair. We propose that Trichinella spiralis controls apoptosis by controlling the time of arrival of new myonucleus from satelite cells in replacement of the damaged one.

5.2 Description of the model

Here we provide short summary of the mathematical model of apoptosis with all modifications and expansions (for biological background see sections 4.2 and 5.1). The dynamics of the model is given by the following biochemical reactions, where k-s are the corresponding kinetic reaction rates as used in the simulations and J-s are corresponding fluxes derived from law of mass action:

Activation of caspase-8 by DISC

$$DISC + PC8 \xrightarrow{k_D} DISC + C8 \qquad k_D = 10\,\mu\mathrm{M}^{-1}\mathrm{s}^{-1}$$

$$J_D = k_D[DISC][PC8]$$

Inhibition of caspase-8 by BAR

$$C8 + BAR \underset{k_B^-}{\overset{k_B^+}{\rightleftharpoons}} C8 \cdot BAR \qquad k_B^+ = 5\,\mu\mathrm{M}^{-1}\mathrm{s}^{-1}$$

$$J_B = k_B^+[C8][BAR] - k_B^-[C8 \cdot BAR] \qquad k_B^- = 0.0035\,\mathrm{s}^{-1}$$

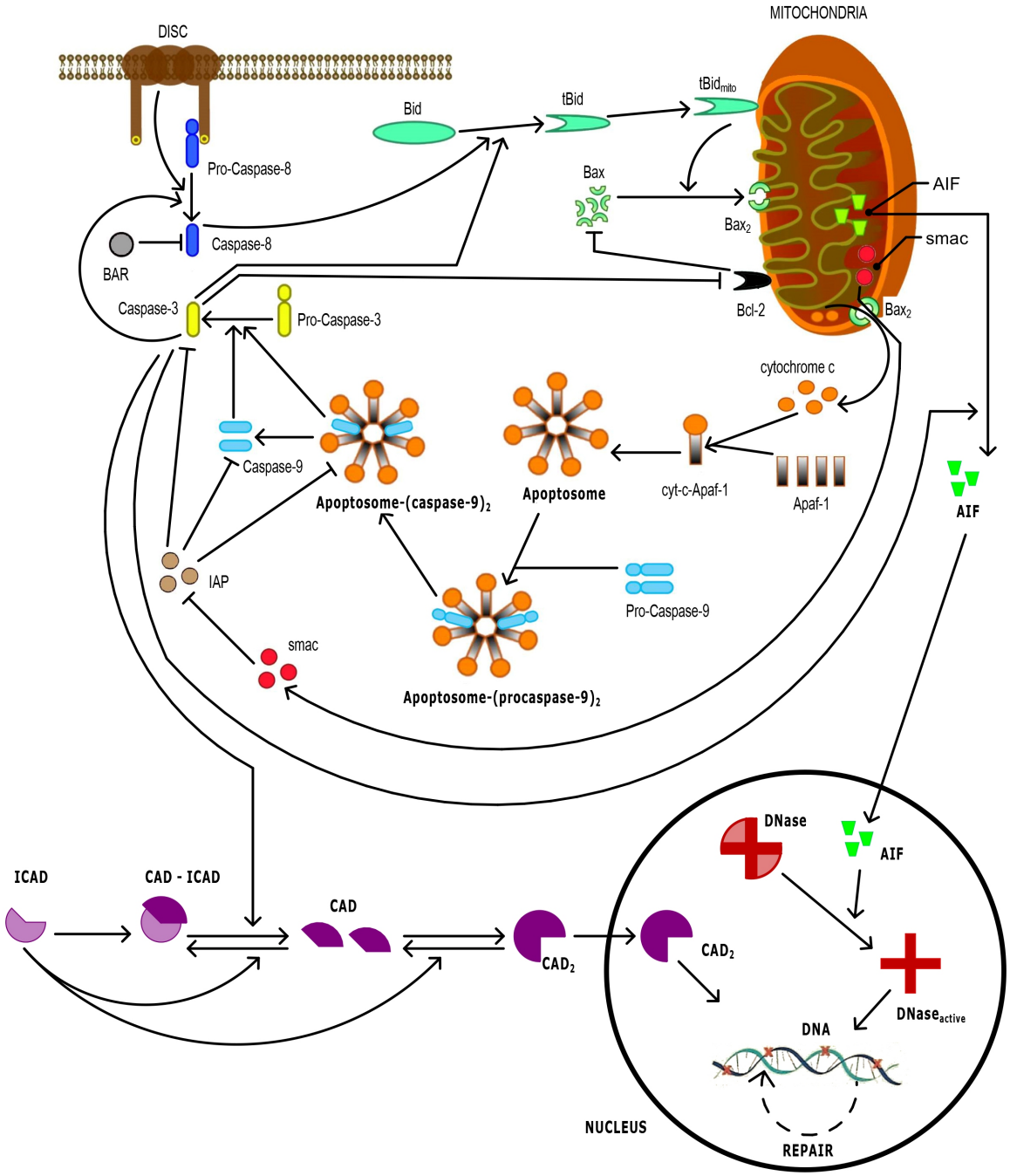

Figure 9: Graphic representation of the expanded model of apoptosis.

Cleavage of Bid by caspase-8

$$C8 + Bid \underset{k_0^-}{\overset{k_0^+}{\rightleftharpoons}} C8 \cdot Bid \qquad k_0^+ = 10\,\mu\mathrm{M}^{-1}\mathrm{s}^{-1}$$

$$J_0 = k_0^+[C8][Bid] - k_0^-[C8 \cdot Bid] \qquad k_0^- = 0.5\,\mathrm{s}^{-1}$$

$$C8 \cdot Bid \xrightarrow{k_0^f} C8 + tBid \qquad k_0^f = 0.1\,\mathrm{s}^{-1}$$

$$J_0^f = k_0^f[C8 \cdot Bid]$$

Translocation of truncated Bid to mitochondrial outer membrane

$$tBid + mit \xrightarrow{k_{11}} tBid_{mito} + mit \qquad k_{11} = 10\,\mathrm{s}^{-1}$$

$$J_{11} = k_{11}[tBid][mit]$$

Formation of Bax_2 channels in mitochondrial membrane

$$tBid_{mito} + Bax \xrightarrow{k_{12}} tBid \cdot Bax \qquad k_{12} = 10\,\mu\mathrm{M}^{-1}\mathrm{s}^{-1}$$

$$J_{12} = k_{12}[tBid_{mito}][Bax]$$

$$tBid \cdot Bax + Bax \xrightarrow{k_{12f}} tBid + Bax_2 \qquad k_{12^f} = 10\,\mu\mathrm{M}^{-1}\mathrm{s}^{-1}$$

$$J_{12^f} = k_{12^f}[tBid \cdot Bax][Bax]$$

Release of cytochrome c from mitochondria to cytoplasm

$$Bax_2 + c_{mito} \xrightarrow{k_{14}} Bax_2 + c \qquad k_{14} = 10\,\mu\mathrm{M}^{-1}\mathrm{s}^{-1}$$

$$J_{14} = k_{14}[Bax_2][c_{mito}]$$

Release of smac from mitochondria to cytoplasm

$$Bax_2 + smac_{mito} \xrightarrow{k_{15}} Bax_2 + smac \qquad k_{15} = 10\,\mu\mathrm{M}^{-1}\mathrm{s}^{-1}$$

$$J_{15} = k_{15}[Bax_2][smac_{mito}]$$

Apoptosome complex formation

$$c + Apaf\text{-}1 \underset{k_{1a}^-}{\overset{k_{1a}^+}{\rightleftharpoons}} c \cdot Apaf\text{-}1 \qquad k_{1a}^+ = 5\,\mu\mathrm{M}^{-1}\mathrm{s}^{-1}$$

$$J_{1a} = k_{1a}^+[c][Apaf\text{-}1] - k_{1a}^-[c \cdot Apaf\text{-}1] \qquad k_{1a}^- = 0.5\,\mathrm{s}^{-1}$$

$$7\,(c \cdot Apaf\text{-}1) \underset{k_{1b}^-}{\overset{k_{1b}^+}{\rightleftharpoons}} apop \qquad k_{1b}^+ = 5 \cdot 104\,\mu\mathrm{M}^{-3}\mathrm{s}^{-1}$$

$$J_{1b} = k_{1b}^+[c \cdot Apaf\text{-}1]^4 - k_{1b}^-[apop] \qquad k_{1b}^- = 0.5\,\mathrm{s}^{-1}$$

Activation of caspase-9 by apoptosome

$$apop + PC9 \underset{k_{2a}^-}{\overset{k_{2a}^+}{\rightleftharpoons}} apop \cdot PC9 \qquad k_{2a}^+ = 10\,\mu\mathrm{M}^{-1}\mathrm{s}^{-1}$$

$$J_{2a} = k_{2a}^+[apop][PC9] - k_{2a}^-[apop \cdot PC9] \qquad k_{2a}^- = 0.5\,\mathrm{s}^{-1}$$

$$apop \cdot PC9 + PC9 \underset{k_{2b}^-}{\overset{k_{2b}^+}{\rightleftharpoons}} apop \cdot PC9 \qquad k_{2b}^+ = 10\,\mu\mathrm{M}^{-1}\mathrm{s}^{-1}$$

$$J_{2b} = k_{2b}^+[apop \cdot PC9][PC9] - k_{2b}^-[apop \cdot (PC9)_2] \qquad k_{2b}^- = 0.5\,\mathrm{s}^{-1}$$

$$apop \cdot (PC9)_2 \xrightarrow{k_3} apop \cdot (C9)_2 \qquad k_3 = 0.1\,\mathrm{s}^{-1}$$

$$J_3 = k_3[apop \cdot (PC9)_2]$$

$$apop \cdot (C9)_2 \underset{k_{4a}^-}{\overset{k_{4a}^+}{\rightleftharpoons}} apop \cdot C9 + C9 \qquad k_{4a}^+ = 5\,\mathrm{s}^{-1}$$

$$J_{4a} = k_{4a}^+[apop \cdot (C9)_2] - k_{4a}^-[apop \cdot C9][C9] \qquad k_{4a}^- = 0.5\,\mu\mathrm{M}^{-1}\mathrm{s}^{-1}$$

$$apop \cdot C9 \underset{k_{4b}^-}{\overset{k_{4b}^+}{\rightleftharpoons}} apop + C9 \qquad k_{4b}^+ = 5\,\mathrm{s}^{-1}$$

$$J_{4b} = k_{4b}^+[apop \cdot C9] - k_{4b}^-[apop][C9] \qquad k_{4b}^- = 0.5\,\mu\mathrm{M}^{-1}\mathrm{s}^{-1}$$

Activation of caspase-3 by caspase-9

$$C9 + PC3 \underset{k_{6a}^-}{\overset{k_{6a}^+}{\rightleftharpoons}} C9 \cdot PC3 \qquad k_{6a}^+ = 10\,\mu\mathrm{M}^{-1}\mathrm{s}^{-1}$$

$$J_{6a} = k_{6a}^+[C9][PC3] - k_{6a}^-[C9 \cdot PC3] \qquad k_{6a}^- = 0.5\,\mathrm{s}^{-1}$$

$$C9 \cdot PC3 \xrightarrow{k_{6a}^f} C9 + C3 \qquad k_{6a}^f = 0.001\,\mathrm{s}^{-1}$$

$$J_{6a}^f = k_{6a}^f[C9 \cdot PC3]$$

Another mechanism of activation of caspase-3

$$apop \cdot (C9)_2 + PC3 \underset{k_{6b}^-}{\overset{k_{6b}^+}{\rightleftharpoons}} apop \cdot (C9)_2 \cdot PC3 \qquad k_{6b}^+ = 10\,\mu\mathrm{M}^{-1}\mathrm{s}^{-1}$$

$$J_{6b} = k_{6b}^+[apop \cdot (C9)_2][PC3] - k_{6b}^-[apop \cdot (C9)_2 \cdot PC3] \qquad k_{6b}^- = 0.5\,\mathrm{s}^{-1}$$

$$apop \cdot (C9)_2 \cdot PC3 \xrightarrow{k_{6b}^f} apop \cdot (C9)_2 + C3 \qquad k_{6b}^f = 0.1\,\mathrm{s}^{-1}$$

$$J_{6b}^f = k_{6b}^f[apop \cdot (C9)_2 \cdot PC3]$$

Loop activation of caspase-8 by caspase-3

$$C3 + PC8 \underset{k_x^-}{\overset{k_x^+}{\rightleftharpoons}} C3 \cdot PC8 \qquad k_x^+ = 10\,\mu\mathrm{M}^{-1}\mathrm{s}^{-1}$$

$$J_x = k_x^+[C3][PC8] - k_x^-[C3 \cdot PC8] \qquad k_x^- = 0.5\,\mathrm{s}^{-1}$$

$$C3 \cdot PC8 \xrightarrow{k_x^f} C3 + C8 \qquad k_x^f = 0.001\,\mathrm{s}^{-1}$$

$$J_x^f = k_x^f[C3 \cdot PC8]$$

Inhibition of caspase-9 by IAP

$$C9 + IAP \underset{k_{5a}^-}{\overset{k_{5a}^+}{\rightleftharpoons}} C9 \cdot IAP \qquad k_{5a}^+ = 5\,\mu\mathrm{M}^{-1}\mathrm{s}^{-1}$$

$$J_{5a} = k_{5a}^+[C9][IAP] - k_{5a}^-[C9 \cdot IAP] \qquad k_{5a}^- = 0.0035\,\mathrm{s}^{-1}$$

$$apop \cdot C9 + IAP \underset{k_{5b}^-}{\overset{k_{5b}^+}{\rightleftharpoons}} apop \cdot C9 \cdot IAP \qquad k_{5b}^+ = 5\,\mu\mathrm{M}^{-1}\mathrm{s}^{-1}$$

$$J_{5b} = k_{5b}^+[apop \cdot C9][IAP] - k_{5b}^-[apop \cdot C9 \cdot IAP] \qquad k_{5b}^- = 0.0035\,\mathrm{s}^{-1}$$

$$apop \cdot (C9)_2 + IAP \underset{k_{5c}^-}{\overset{k_{5c}^+}{\rightleftharpoons}} apop \cdot (C9)_2 \cdot IAP \qquad k_{5c}^+ = 5\,\mu\mathrm{M}^{-1}\mathrm{s}^{-1}$$

$$J_{5c} = k_{5c}^+[apop \cdot (C9)_2][IAP] - k_{5c}^-[apop \cdot (C9)_2 \cdot IAP] \qquad k_{5c}^- = 0.0035\,\mathrm{s}^{-1}$$

Inhibition of caspase-3 by IAP

$$C3 + IAP \underset{k_7^-}{\overset{k_7^+}{\rightleftharpoons}} C3 \cdot IAP \qquad k_7^+ = 5\,\mu\mathrm{M}^{-1}\mathrm{s}^{-1}$$

$$J_7 = k_7^+[C3][IAP] - k_7^-[C3 \cdot IAP] \qquad k_7^- = 0.0035\,\mathrm{s}^{-1}$$

Inhibition of IAP by smac

$$IAP + smac \underset{k_{SM}^-}{\overset{k_{SM}^+}{\rightleftharpoons}} IAP \cdot smac \qquad k_{SM}^+ = 5\,\mu\mathrm{M}^{-1}\mathrm{s}^{-1}$$

$$J_{SM} = k_{SM}^+[IAP][smac] - k_{SM}^-[IAP \cdot smac] \qquad k_{SM}^- = 0.0035\,\mathrm{s}^{-1}$$

Loop cleavage of Bid by caspase-3

$$C3 + Bid \underset{k_8^-}{\overset{k_8^+}{\rightleftharpoons}} C3 \cdot Bid \qquad k_8^+ = 10\,\mu\mathrm{M}^{-1}\mathrm{s}^{-1}$$

$$J_8 = k_8^+[C3][Bid] - k_8^-[C3 \cdot Bid] \qquad k_8^- = 0.5\,\mathrm{s}^{-1}$$

$$C3 \cdot Bid \xrightarrow{k_8^f} C3 + tBid \qquad k_8^f = 0.1\,\mathrm{s}^{-1}$$

$$J_8^f = k_8^f[C3 \cdot Bid]$$

Inhibition of Bax by Bcl-2

$$Bax + Bcl\text{-}2 \xrightarrow{k_{13}} (Bax \cdot Bcl\text{-}2)_{inactive} \qquad k_{13} = 10\,\mu\mathrm{M}^{-1}\mathrm{s}^{-1}$$

$$J_{13} = k_{13}[Bax][Bcl\text{-}2]$$

Cleavage of Bcl-2 by caspase-3

$$C3 + Bcl\text{-}2 \underset{k_9^-}{\overset{k_9^+}{\rightleftharpoons}} C3 \cdot Bcl\text{-}2 \qquad k_9^+ = 10\,\mu\mathrm{M}^{-1}\mathrm{s}^{-1}$$

$$J_9 = k_9^+[C3][Bcl\text{-}2] - k_9^-[C3 \cdot Bcl\text{-}2] \qquad k_9^- = 0.5\,\mathrm{s}^{-1}$$

$$C3 \cdot Bcl\text{-}2 \xrightarrow{k_9^f} C3 + Bcl\text{-}2_{cleaved} \qquad k_9^f = 0.1\,\mathrm{s}^{-1}$$

$$J_9^f = k_9^f[C3 \cdot Bcl\text{-}2]$$

Release of AIF from mitochondria to cytoplasm

$$C3 + AIF_{mito} \xrightarrow{k_{20}} C3 + AIF \qquad k_{20} = 1\,\mu\mathrm{M}^{-1}\mathrm{s}^{-1}$$

$$J_{20} = k_{20}[C3][AIF_{mito}]$$

Translocation of AIF from cytoplasm to nucleus

$$AIF \xrightarrow{k_{21}} AIF_{nuc} \qquad k_{21} = 10\,\mathrm{s}^{-1}$$

$$J_{21} = k_{21}[AIF]$$

Activation of DNase by AIF in nucleus

$$AIF_{nuc} + DNase \underset{k_{22}^-}{\overset{k_{22}^+}{\rightleftharpoons}} AIF \cdot DNase \qquad k_{22}^+ = 10\,\mu\mathrm{M}^{-1}\mathrm{s}^{-1}$$

$$J_{22} = k_{22}^+[AIF_{nuc}][DNase] - k_{22}^-[AIF \cdot DNase] \qquad k_{22}^- = 0.5\,\mathrm{s}^{-1}$$

$$AIF \cdot DNase \xrightarrow{k_{22}^f} AIF_{nuc} + DNase_{active} \qquad k_{22}^f = 0.1\,\mathrm{s}^{-1}$$

$$J_{22}^f = k_{22}^f[AIF \cdot DNase]$$

Fragmentation of DNA by active DNase

$$DNA + DNase_{active} \xrightarrow{k_{23}} DNA + DNA_{damaged} + DNase_{active} \qquad k_{23} = 0.5\,\mu\mathrm{M}^{-1}\mathrm{s}^{-1}$$

$$J_{23} = k_{23} \cdot F([DNA]; \alpha_{23}, \beta_{23}) \cdot [DNase_{active}] \qquad \alpha_{23} = 6, \beta_{23} = 5$$

where function F is a cumulative distribution function of beta distribution with shape parameters α_{23} and β_{23} defined by (5.2).

Activation of CAD by cleaving ICAD in CAD·ICAD complex at site Asp^{117} by caspase-3

$$C3 + CAD \cdot ICAD \underset{k_{24a}^-}{\overset{k_{24a}^+}{\rightleftharpoons}} CAD \cdot ICAD \cdot C3 \qquad k_{24a}^+ = 10\,\mu\mathrm{M}^{-1}\mathrm{s}^{-1}$$

$$J_{24a} = k_{24a}^+[C3][CAD \cdot ICAD] \qquad k_{24a}^- = 0.5\,\mathrm{s}^{-1}$$
$$- k_{24a}^-[CAD \cdot ICAD \cdot C3]$$

$$CAD \cdot ICAD \cdot C3 \xrightarrow{k_{24a}^f} C3 + CAD \qquad k_{24a}^f = 0.1\,\mathrm{s}^{-1}$$

$$J_{24a}^f = k_{24a}^f[CAD \cdot ICAD \cdot C3]$$

Activation of CAD by first cleaving ICAD in CAD·ICAD complex at site Asp^{224} and then at site Asp^{117} by caspase-3

$$C3 + CAD \cdot ICAD \underset{k^-_{24a}}{\overset{k^+_{24a}}{\rightleftharpoons}} CAD \cdot ICAD \cdot C3 \qquad k^+_{24a} = 10\,\mu\mathrm{M}^{-1}\mathrm{s}^{-1}$$

$$J_{24a} = k^+_{24a}[C3][CAD \cdot ICAD] \qquad k^-_{24a} = 0.5\,\mathrm{s}^{-1}$$
$$- k^-_{24a}[CAD \cdot ICAD \cdot C3]$$

$$CAD \cdot ICAD \cdot C3 \xrightarrow{k^f_{24a}} C3 + CAD \cdot IACD_{Asp^{224}} \qquad k^f_{24a} = 0.1\,\mathrm{s}^{-1}$$

$$J^f_{24a} = k^f_{24a}[CAD \cdot ICAD \cdot C3]$$

$$C3 + CAD \cdot IACD_{Asp^{224}} \underset{k^-_{24b}}{\overset{k^+_{24b}}{\rightleftharpoons}} CAD \cdot ICAD_{Asp^{224}} \cdot C3 \qquad k^+_{24b} = 10\,\mu\mathrm{M}^{-1}\mathrm{s}^{-1}$$

$$J_{24b} = k^+_{24b}[C3][CAD \cdot ICAD_{Asp^{224}}] \qquad k^-_{24b} = 0.5\,\mathrm{s}^{-1}$$
$$- k^-_{24b}[CAD \cdot ICAD_{Asp^{224}} \cdot C3]$$

$$CAD \cdot ICAD_{Asp^{224}} \cdot C3 \xrightarrow{k^f_{24b}} C3 + CAD \qquad k^f_{24b} = 0.1\,\mathrm{s}^{-1}$$

$$J^f_{24b} = k^f_{24b}[CAD \cdot ICAD_{Asp^{224}} \cdot C3]$$

Inhibition of CAD by ICAD

$$CAD + ICAD \xrightarrow{k_{25}} CAD \cdot ICAD \qquad k_{25} = 0.1\,\mu\mathrm{M}^{-1}\mathrm{s}^{-1}$$

$$J_{25} = k_{25}[CAD][ICAD]$$

Dimerisation of CAD

$$2CAD \xrightarrow{k_{26}} CAD_2 \qquad k_{26} = 10\,\mu\mathrm{M}^{-1}\mathrm{s}^{-1}$$

$$J_{26} = k_{26}[CAD]^2$$

Dissocioation of CAD_2 dimers by ICAD

$$CAD_2 + ICAD \xrightarrow{k_{27}} 2CAD + ICAD \qquad k_{27} = 0.1\,\mu\mathrm{M}^{-1}\mathrm{s}^{-1}$$

$$J_{27} = k_{27}[CAD_2][ICAD]$$

Translocation of CAD_2 dimers from cytoplasm to nucleus

$$CAD_2 \xrightarrow{k_{28}} CAD_{2,nuc} \qquad k_{28} = 10\,\mathrm{s}^{-1}$$

$$J_{28} = k_{28}[CAD_2]$$

Fragmentation of DNA by nuclear CAD_2 dimer

$$DNA + CAD_{2,nuc} \xrightarrow{k_{29}} DNA + DNA_{damaged} + CAD_{2,nuc} \qquad k_{29} = 0.5\,\mu\mathrm{M}^{-1}\mathrm{s}^{-1}$$

$$J_{29} = k_{29} \cdot \hat{f}\left([DNA]; \alpha_{29}, \beta_{29}\right) \cdot [CAD_{2,nuc}] \qquad \alpha_{29} = 3, \beta_{29} = 2$$

where function $\hat{f}$ is the probability density function of Beta distribution with shape parameters α_{29} and β_{29} normalised so that the maximum is one and is defined by the (5.4).

Self-repair of DNA

$$DNA + DNA_{damaged} \xrightarrow{k_{30}} DNA \qquad k_{30} = 0.001\,\mu\mathrm{M}^{-1}\mathrm{s}^{-1}$$

$$J_{30} = k_{30} \cdot \hat{f}([DNA]; \alpha_{30}, \beta_{30}) \qquad \alpha_{30} = 2, \beta_{30} = 10$$

where function $\hat{f}$ is the probability density function of Beta distribution with shape parameters α_{29} and β_{29} normalised so that the maximum is one and is defined by the (5.4).

Reduction of mitochondrial activity by Bax_2 channels

$$mit + Bax_2 \xrightarrow{k_{31}} mit + mit_{inactive} + Bax_2 \qquad k_{31} = 0.001\,\mathrm{s}^{-1}$$

$$J_{31} = k_{31}\frac{[Bax_2]}{M_{Bax_2}}[mit] \qquad M_{Bax_2} = 0.052\,\mu\mathrm{M}$$

where M_{Bax_2} is the maximal concentration of Bax_2 channels on mitochondrial outer membrane.

Increase in mitochondrial activity in absence of Bax_2 channels

$$mit + mit_{inactive} \xrightarrow{k_{32}} mit \qquad k_{32} = 0.01\,\mathrm{s}^{-1}$$

$$J_{32} = k_{32}\left(1 - \frac{[Bax_2]}{M_{Bax_2}}\right)(1 - [mit]) \qquad M_{Bax_2} = 0.052\,\mu\mathrm{M}$$

where M_{Bax_2} is the maximal concentration of Bax_2 channels on mitochondrial outer membrane.

Synthesis and degradation of molecules

The initial concentrations of all compounds are set to their homoeostatic levels, that is to their equilibrium values in the absence of apoptotic signal. For DNA and mitochondrial activity, mit, this level is 1. $DISC$ again serves as an initial apoptotic signal with the initial strength $10^{-5}\,\mu$M.

$$DNA \xrightarrow{\Omega_{PC8}} PC8 \qquad \Omega_{PC8} = 6 \cdot 10^{-4}\,\mu\mathrm{Ms}^{-1}$$
$$DNA \xrightarrow{\Omega_{BAR}} BAR \qquad \Omega_{BAR} = 3 \cdot 10^{-5}\,\mu\mathrm{Ms}^{-1}$$
$$DNA \xrightarrow{\Omega_{Bid}} Bid \qquad \Omega_{Bid} = 6 \cdot 10^{-5}\,\mu\mathrm{Ms}^{-1}$$
$$DNA \xrightarrow{\Omega_{Bax}} Bax \qquad \Omega_{Bax} = 5 \cdot 10^{-4}\,\mu\mathrm{Ms}^{-1}$$
$$mit \xrightarrow{\Omega_{c_{mito}}} c_{mito} \qquad \Omega_{c_{mito}} = 5 \cdot 10^{-4}\,\mu\mathrm{Ms}^{-1}$$
$$mit \xrightarrow{\Omega_{smac_{mito}}} smac_{mito} \qquad \Omega_{smac_{mito}} = 5 \cdot 10^{-4}\,\mu\mathrm{Ms}^{-1}$$
$$DNA \xrightarrow{\Omega_{Apaf\text{-}1}} Apaf\text{-}1 \qquad \Omega_{Apaf\text{-}1} = 6 \cdot 10^{-4}\,\mu\mathrm{Ms}^{-1}$$
$$DNA \xrightarrow{\Omega_{PC9}} PC9 \qquad \Omega_{PC9} = 6 \cdot 10^{-4}\,\mu\mathrm{Ms}^{-1}$$
$$DNA \xrightarrow{\Omega_{PC3}} PC3 \qquad \Omega_{PC3} = 6 \cdot 10^{-4}\,\mu\mathrm{Ms}^{-1}$$
$$DNA \xrightarrow{\Omega_{IAP}} IAP \qquad \Omega_{IAP} = 3 \cdot 10^{-5}\,\mu\mathrm{Ms}^{-1}$$
$$mit \xrightarrow{\Omega_{Bcl\text{-}2}} Bcl\text{-}2 \qquad \Omega_{Bcl\text{-}2} = 10^{-5}\,\mu\mathrm{Ms}^{-1}$$
$$mit \xrightarrow{\Omega_{AIF_{mito}}} AIF_{mito} \qquad \Omega_{AIF_{mito}} = 3 \cdot 10^{-4}\,\mu\mathrm{Ms}^{-1}$$
$$DNA \xrightarrow{\Omega_{DNase}} DNase \qquad \Omega_{DNase} = 5 \cdot 10^{-5}\,\mu\mathrm{Ms}^{-1}$$
$$DNA \xrightarrow{\Omega_{ICAD}} ICAD \qquad \Omega_{ICAD} = 6 \cdot 10^{-4}\,\mu\mathrm{Ms}^{-1}$$
$$DNA + ICAD \xrightarrow{\Omega_{CAD}} CAD \cdot ICAD \qquad \Omega_{CAD} = 6 \cdot 10^{-4}\,\mathrm{s}^{-1}$$

A first order degradation kinetics with a uniform rate constant of $\mu = 0.004$ is adopted for all compounds except for DNA and mit that do not degrade and $DISC$ that after serving as initial apoptotic signal quickly degrades at constant rate $\mu_{DISC} = 100\mu$.

Since DNA does not degrade but only fragment the overall amount of DNA is constant thorough simulation: $DNA{+}DNA_{damaged} = const.$ o we propose new variable DFI, DNA fragmentation index, that will measure the degree of fragmentation of DNA and thus decrease in synthetic activity of DNA too, with the following relations to the states of DNA: $[DNA] = [DNA]_0 - [DFI]$ and $[DNA_{damaged}] = [DFI]$.

The above biochemical reactions translate into the following system of ordinary differential equations:

$$\dot{[DISC]} = -100\mu[DISC] \tag{5.6}$$

$$\dot{[PC8]} = \Omega_{PC8}(1-[DFI]) - \mu[PC8] - J_D - J_x \tag{5.7}$$

$$\dot{[C8]} = -\mu[C8] + J_D + J_x^f - J_B - J_0 + J_0^f \tag{5.8}$$

$$\dot{[BAR]} = \Omega_{BAR}(1-[DFI]) - \mu[BAR] - J_B \tag{5.9}$$

$$\dot{[C8 \cdot BAR]} = -\mu[C8 \cdot BAR] + J_B \tag{5.10}$$

$$\dot{[Bid]} = \Omega_{Bid}(1-[DFI]) - \mu[Bid] - J_0 - J_8 \tag{5.11}$$

$$\dot{[C8 \cdot Bid]} = -\mu[C8 \cdot Bid] + J_0 - J_0^f \tag{5.12}$$

$$\dot{[tBid]} = -\mu[tBid] + J_0^f + J_8^f - J_{11} + J_{12b} \tag{5.13}$$

$$\dot{[tBid_{mito}]} = -\mu[tBid_{mito}] + J_{11} - J_{12a} \tag{5.14}$$

$$\dot{[Bax]} = \Omega_{Bax}(1-[DFI]) - \mu[Bax] - J_{12a} - J_{12b} - J_{13} \tag{5.15}$$

$$\dot{[tBid \cdot Bax]} = -\mu[tBid \cdot Bax] + J_{12a} - J_{12b} \tag{5.16}$$

$$\dot{[Bax_2]} = -\mu[Bax_2] + J_{12b} + dmit[Bax_2] \tag{5.17}$$

$$\dot{[c_{mito}]} = \Omega_{c_{mito}}[mit] - \mu[c_{mito}] - J_{14} \tag{5.18}$$

$$\dot{[c]} = -\mu[c] + J_{14} - J_{1a} \tag{5.19}$$

$$\dot{[smac_{mito}]} = \Omega_{smac_{mito}}[mit] - \mu[smac_{mito}] - J_{15} \tag{5.20}$$

$$\dot{[smac]} = -\mu[smac] + J_{15} - J_{SM} \tag{5.21}$$

$$\dot{[Apaf\text{-}1]} = \Omega_{Apaf\text{-}1}(1-[DFI]) - \mu[Apaf\text{-}1] - J_{1a} \tag{5.22}$$

$$\dot{[c \cdot Apaf\text{-}1]} = -\mu[c \cdot Apaf\text{-}1] + J_{1a} - 7J_{1b} \tag{5.23}$$

$$\dot{[apop]} = -\mu[apop] + J_{1b} - J_{2a} + J_{4b} \tag{5.24}$$

$$\dot{[PC9]} = \Omega_{PC9}(1-[DFI]) - \mu[PC9] - J_{2a} - J_{2b} \tag{5.25}$$

$$\dot{[apop \cdot PC9]} = -\mu[apop \cdot PC9] + J_{2a} - J_{2b} \tag{5.26}$$

$$\dot{[apop \cdot (PC9)_2]} = -\mu[apop \cdot (PC9)_2] + J_{2b} - J_3 \tag{5.27}$$

$$\dot{[apop \cdot (C9)_2]} = -\mu[apop \cdot (C9)_2] + J_3 - J_{4a} - J_{5c} - J_{6b} + J_{6b}^f \tag{5.28}$$

$$\dot{[apop \cdot C9]} = -\mu[apop \cdot C9] + J_{4a} - J_{4b} - J_{5b} \tag{5.29}$$

$$\dot{[C9]} = -\mu[C9] + J_{4a} + J_{4b} - J_{5a} - J_{6a} + J_{6a}^f \tag{5.30}$$

$$\dot{[PC3]} = \Omega_{PC3}(1-[DFI]) - \mu[PC3] - J_{6a} - J_{6b} \tag{5.31}$$

$$[C9 \cdot \dot{PC3}] = -\mu[C9 \cdot PC3] + J_{6a} - J_{6a}^f \tag{5.32}$$

$$[apop \cdot (\dot{C9})_2 \cdot PC3] = -\mu[apop \cdot (C9)_2 \cdot PC3]] + J_{6b} - J_{6b}^f \tag{5.33}$$

$$\begin{aligned}[\dot{C3}] &= -\mu[C3] + J_{6a}^f + J_{6b}^f - J_7 - J_x + J_x^f \\ &\quad - J_8 + J_8^f - J_9 + J_9^f - J_{24a} + J_{24a}^f - J_{24b} + J_{24b}^f\end{aligned} \tag{5.34}$$

$$[C3 \cdot \dot{PC8}] = -\mu[C3 \cdot PC8] + J_x - J_x^f \tag{5.35}$$

$$\begin{aligned}[\dot{IAP}] &= \Omega_{IAP}(1 - [DFI]) - \mu[IAP] - J_{5a} - J_{5b} - J_{5c} \\ &\quad - J_7 - J_{SM}\end{aligned} \tag{5.36}$$

$$[C9 \cdot \dot{IAP}] = -\mu[C9 \cdot IAP] + J_{5a} \tag{5.37}$$

$$[apop \cdot \dot{C9} \cdot IAP] = -\mu[apop \cdot C9 \cdot IAP] + J_{5b} \tag{5.38}$$

$$[apop \cdot (\dot{C9})_2 \cdot IAP] = -\mu[apop \cdot (C9)_2 \cdot IAP] + J_{5c} \tag{5.39}$$

$$[C3 \cdot \dot{IAP}] = -\mu[C3 \cdot IAP] + J_7 \tag{5.40}$$

$$[IAP \cdot \dot{smac}] = -\mu[IAP \cdot smac] + J_{SM} \tag{5.41}$$

$$[C3 \cdot \dot{Bid}] = -\mu[C3 \cdot Bid] + J_8 - J_8^f \tag{5.42}$$

$$[\dot{Bcl\text{-}2}] = \Omega_{Bcl\text{-}2}[mit] - \mu[Bcl\text{-}2] - J_{13} - J_9 \tag{5.43}$$

$$[Bax \cdot \dot{Bcl\text{-}2}] = -\mu[Bax \cdot Bcl\text{-}2] + J_{13} \tag{5.44}$$

$$[C3 \cdot \dot{Bcl\text{-}2}] = -\mu[C3 \cdot Bcl\text{-}2] + J_9 - J_9^f \tag{5.45}$$

$$[\dot{Bcl\text{-}2_{cleaved}}] = -\mu[Bcl\text{-}2_{cleaved}] + J_9^f \tag{5.46}$$

$$[\dot{AIF}_{mito}] = \Omega_{AIF_{mito}}[mit] - \mu[AIF_{mito}] - J_{20} \tag{5.47}$$

$$[\dot{AIF}] = -\mu[AIF] + J_{20} - J_{21} \tag{5.48}$$

$$[\dot{AIF}_{nuc}] = -\mu[AIF_{nuc}] + J_{21} - J_{22} + J_2 2^f \tag{5.49}$$

$$[\dot{DNase}] = \Omega_{DNase}(1 - [DFI]) - \mu[DNase] - J_{22} \tag{5.50}$$

$$[AIF \cdot \dot{DNase}] = -\mu[AIF \cdot DNase] + J_{22} - J_{22}^f \tag{5.51}$$

$$[\dot{DNase_{active}}] = -\mu[DNase_{active}] + J_{22}^f \tag{5.52}$$

$$\begin{aligned}[\dot{ICAD}] &= \Omega_{ICAD}(1 - [DFI]) - \mu[ICAD] - J_{25} \\ &\quad - \Omega_{CAD}(1 - [DFI])[ICAD]\end{aligned} \tag{5.53}$$

$$\begin{aligned}[CAD \cdot \dot{ICAD}] &= \Omega_{CAD}(1 - [DFI])[ICAD] - \mu[CAD \cdot ICAD] \\ &\quad - J_{24a} + J_{25}\end{aligned} \tag{5.54}$$

$$[\dot{CAD \cdot ICAD \cdot C3}] = -\mu[CAD \cdot ICAD \cdot C3] + J_{24a} - J^f_{24a} \tag{5.55}$$

$$[\dot{CAD \cdot ICAD_{Asp^{224}}}] = -\mu[CAD \cdot ICAD_{Asp^{224}}] + \frac{1}{2}J^f_{24a} - J_{24b} \tag{5.56}$$

$$[\dot{CAD \cdot ICAD_{Asp^{224}} \cdot C3}] = -\mu[CAD \cdot ICAD_{Asp^{224}} \cdot C3] + J_{24b} - J^f_{24b} \tag{5.57}$$

$$[\dot{CAD}] = -\mu[CAD] + \frac{1}{2}J^f_{24a} + J^f_{24b} - J_{25} - 2J_{26} + 2J_{27} \tag{5.58}$$

$$[\dot{CAD_2}] = -\mu[CAD_2] + J_{26} - J_{27} - J_{28} \tag{5.59}$$

$$[\dot{CAD_{2,nuc}}] = -\mu[CAD_{2,nuc}] + J_{28} \tag{5.60}$$

$$[\dot{DFI}] = J_{23} + J_{29} - J_{30} \tag{5.61}$$

$$[\dot{mit}] = -J_{31} + J_{32} \tag{5.62}$$

where Ω_X is the production rate of the molecule X, μ is decomposition rate and is the same for all substances, k-s are the kinetic reaction rates given above with the related reactions and J-s are the fluxes defined above with the related biochemical reactions derived according to law of mass action.

5.3 Reduction of the model

System (5.6) – (5.62) consists of 57 ordinary differential equations with 95 parameters most of which are not experimentally verified, making it impractical for quantitative analysis. Therefore we proceed to reduction of the system (5.6) – (5.62). Since $DISC$ does not form complexes with other compounds and only degrades, we can analytically compute concentration of $DISC$ as a function of time: $[DISC](t) = \mathrm{e}^{-100\mu t}$. To further reduce the system we either omitted compounds or reactions, or approximated compounds using quasi-steady-state approximation.

Quasi-steady-state approximation is widely used tool for reduction of systems of ordinary differential equations. It is based on assumption that after fast transient initial phase, the trajectory of the system close enough to the regime where dynamics of the system is driven only by a subset of variables while other change slowly compared to them. This provides justification for formally setting time derivatives of these variables to zero and by solving the system of algebraic equations approximate slowly changing variables. Thus reducing the dimension of the system.

After each step during the reduction of the system (5.6) – (5.62) we verified validity

of each omission or approximation by comparing evolution of concentrations of selected variables after the reduction to those from the model with full dynamics and assessed whether the change is significant (from the qualitative perspective) or not for three different scenarios:

1. for the level of initial apoptotic signal that was did not cause apoptosis in the full system (5.6) – (5.62),

2. for the instance when arrival of the new nucleus did not caused re-start of apoptosis (time of arrival was set to 5000 s after the invasion of Trichinella spiralis) and

3. for the instance when arrival of the new nucleus did cause the initiation of the apoptosis (time of arrival was set to 3000 s after the invasion of Trichinella spiralis).

From the reductions made we can conclude that under given values of parameters anti-apoptotic proteins IAP and Bcl-2 did not have significant influence on the dynamics of the system since their concentrations were low due to high inhibitory effects of *smac* and caspase-3 and thus could be omitted from the model. Similarly, activation of caspase-3 by complex consisting of apoptosome and two active caspase-9 molecules had no significant effect on overall dynamics.

We were able to significantly reduce dynamics of the proposed model (originally there were 57 variables, after reductions only 25 variables are left), while preserving qualitative behaviour of the system. The cumulative effect of reduction can be seen in Figure 10. The most notable changes are:

- bigger decrease in concentration of cytochrome c after the rapid release from mitochondria after initiation of apoptosis and

- quicker dynamics, i.e. quicker initiation and completion of apoptosis (this is expected consequence of using quasi-steady-state approximation).

Graphical representation of the model proposed in section 5.2 after the reductions can be seen in Figure 11. The dynamics of the model proposed in section 5.2 after the reductions can be summarised by the following biochemical reactions where k-s are the

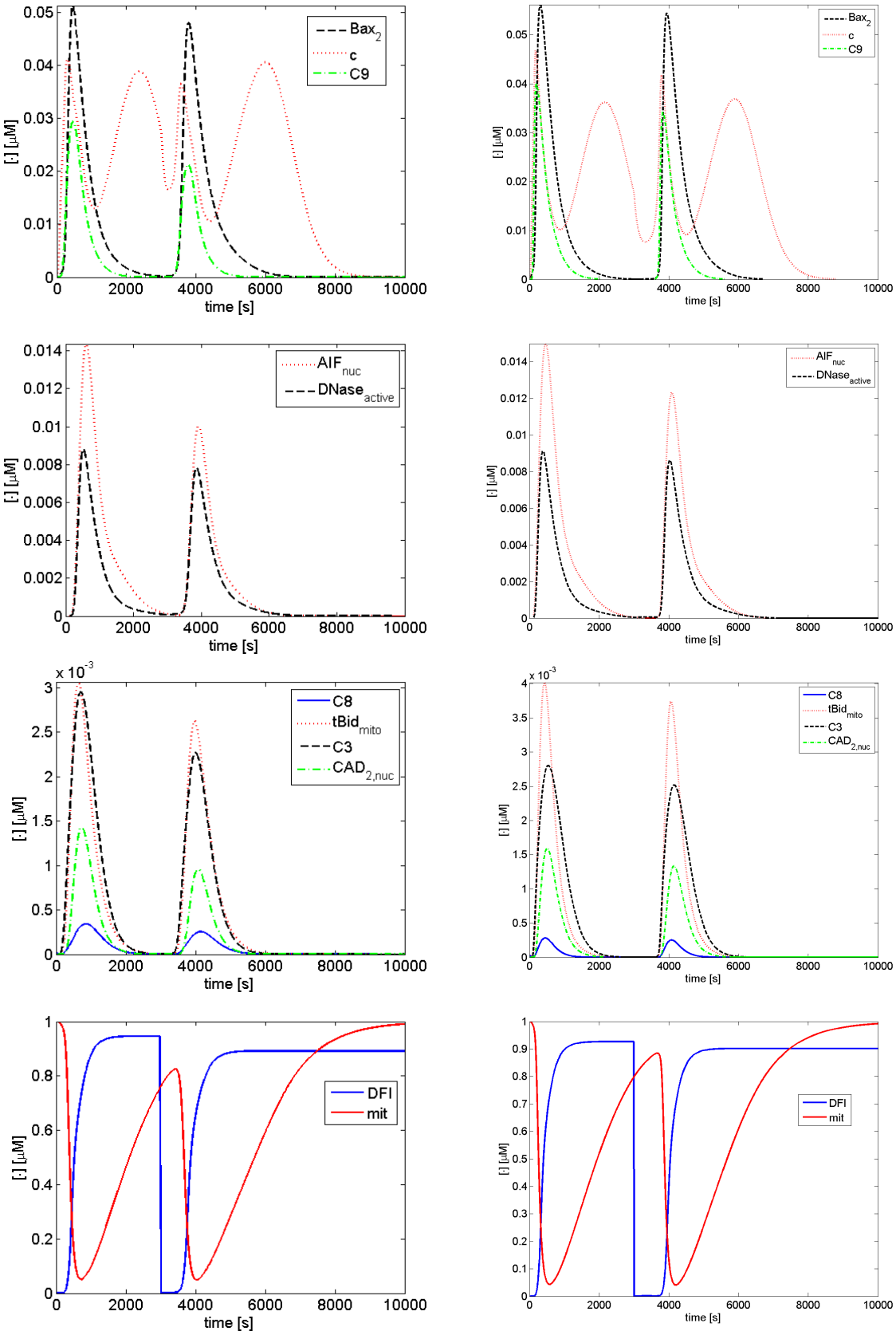

Figure 10: Time evolution of concentrations of selected proteins for model with full dynamics (left) and reduced dynamics (right).

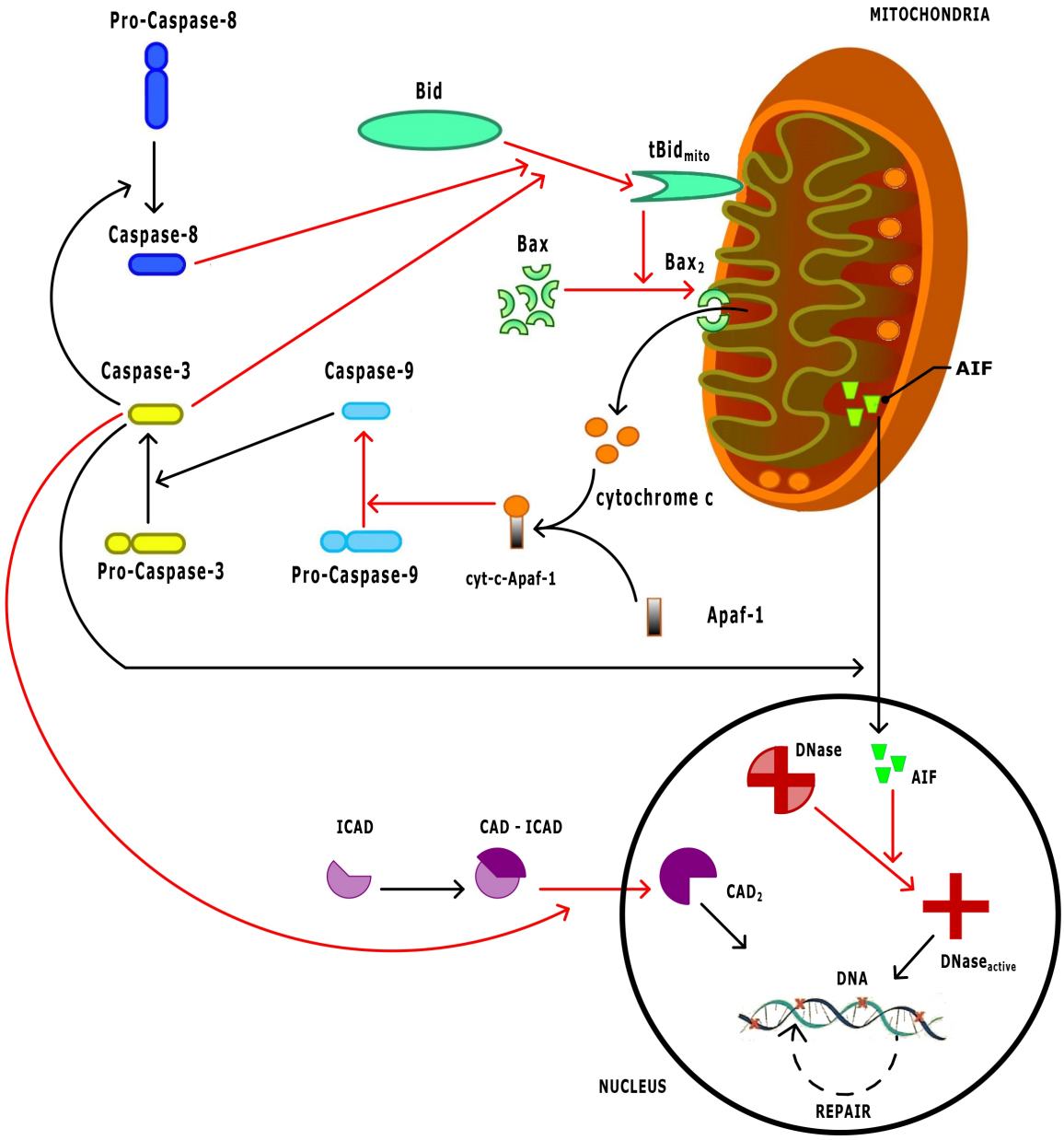

Figure 11: Graphic representation of the expanded model of apoptosis after reductions. Red arrow means that intermediate compounds in the originally assumed kinetic reaction schemes were approximated using quasi-steady state approximation.

kinetic reaction rates of the the original model and J-s are the fluxes:

Cleavage of Bid by caspase-8 and subsequent translocation to mitochondrial outer membrane:

$$C8 + Bid \rightarrow C8 + tBid_{mito}$$

$$J_0 = \frac{k_0^+(\mu + k_0^f)[C8][Bid]}{\mu + k_0^- + k_0^f}$$

$$J_0^f = \frac{k_0^+ k_0^f [C8][Bid]}{\mu + k_0^- + k_0^f}$$

Formation of Bax_2 channels in mitochondrial membrane:

$$tBid_{mito} + 2Bax \rightarrow tBid_{mito} + Bax_2$$

$$J_{12} = k_1 2[tBid_{mito}][Bax]$$

$$J_{12}^f = \frac{k_{12} k_{12}^f [tBid_{mito}][Bax]^2}{\mu + k_1 2^f [Bax]}$$

Release of cytochrome c from mitochondria to cytoplasm:

$$Bax_2 + c_{mito} \xrightarrow{k_{14}} Bax_2 + c \qquad k_{14} = 10\,\mu\mathrm{M}^{-1}\mathrm{s}^{-1}$$

$$J_{14} = k_{14}[Bax_2][c_{mito}]$$

Activation of caspase-9 by seven cytochromes c and Apaf-1 molecules:

$$c + Apaf\text{-}1 \underset{k_{1a}^-}{\overset{k_{1a}^+}{\rightleftharpoons}} c \cdot Apaf\text{-}1 \qquad k_{1a}^+ = 5\,\mu\mathrm{M}^{-1}\mathrm{s}^{-1}$$

$$J_{1a} = k_{1a}^+[c][Apaf\text{-}1] - k_{1a}^-[c \cdot Apaf\text{-}1] \qquad k_{1a}^- = 0.5\,\mathrm{s}^{-1}$$

$$7c \cdot Apaf\text{-}1 + 2PC9 \longrightarrow 7c \cdot Apaf\text{-}1 + 2C9$$

$$J_{1b} = k_{1b}^+[c \cdot Apaf\text{-}1]^7 - k_{1b}^-[apop]$$

$$J_{2a} = k_{2a}^+[apop][PC9] - k_{2a}^-[apop \cdot PC9]$$

$$J_{2b} = k_{2b}^+[apop \cdot PC9][PC9] - k_{2b}^-[apop \cdot (PC9)_2]$$

$$J_{4a} = k_{4a}^+[apop \cdot (C9)_2] - k_{4a}^-[apop \cdot C9][C9]$$

$$J_{4b} = k_{4b}^+[apop \cdot C9] - k_{4b}^-[apop][C9]$$

where:

$$[apop \cdot (C9)_2] = \frac{k_3 A \cdot B \cdot C + k_3 A \cdot B \cdot D \cdot E + k_{4a}^- E[C9]}{\mu - k_3 A \cdot B \cdot D \cdot F + k_{4a}^+ - k_{4a}^- F[C9] + k_{6b}^+[PC3] - k_{6b}^- G - k_{6b}^f G}$$

$$
\begin{aligned}
[apop \cdot C9] &= E + F[apop \cdot (C9)_2] \\
[apop] &= C + D[apop \cdot C9] \\
[apop \cdot PC9] &= B[apop] \\
[apop \cdot (PC9)_2] &= A[apop \cdot PC9] \\
A &= \frac{k_{2b}^{+}[PC9]}{mu + k_{2b}^{-} + k_3} \\
B &= \frac{k_{2a}^{+}[PC9]}{\mu + k_{2a}^{-} + k_{2b}^{+}[PC9] - k_{2b}^{-}A} \\
C &= \frac{k_{1b}^{+}[c \cdot Apaf]^7}{\mu + k_{1b}^{-} + k_{2a}^{+}[PC9] - k_{2a}^{-}[B] + k_{4b}^{-}[C9]} \\
D &= \frac{k_{4b}^{+}}{\mu + k_{1b}^{-} + k_{2a}^{+}[PC9] - k_{2a}^{-}[B] + k_{4b}^{-}[C9]} \\
E &= \frac{k_4 b^{-} C[C9]}{\mu + k_{4a}^{-}[C9] + k_{4b}^{+} - k_{4b}^{-}D[C9]} \\
F &= \frac{k_{4a}^{+}}{\mu + k_{4a}^{-}[C9] + k_{4b}^{+} - k_{4b}^{-}D[C9]} \\
G &= \frac{k_{6b}^{+}[PC3]}{\mu + k_{6b}^{-} + k_{6b}^{f}}
\end{aligned}
$$

Activation of caspase-3 by caspase-9:

$$
\begin{aligned}
C9 + PC3 &\underset{k_{6a}^{-}}{\overset{k_{6a}^{+}}{\rightleftharpoons}} C9 \cdot PC3 & k_{6a}^{+} &= 10\,\mu\mathrm{M}^{-1}\mathrm{s}^{-1} \\
J_{6a} &= k_{6a}^{+}[C9][PC3] - k_{6a}^{-}[C9 \cdot PC3] & k_{6a}^{-} &= 0.5\,\mathrm{s}^{-1}
\end{aligned}
$$

$$
\begin{aligned}
C9 \cdot PC3 &\xrightarrow{k_{6a}^{f}} C9 + C3 & k_{6a}^{f} &= 0.001\,\mathrm{s}^{-1} \\
J_{6a}^{f} &= k_{6a}^{f}[C9 \cdot PC3]
\end{aligned}
$$

Loop activation of caspase-8 by caspase-3:

$$
\begin{aligned}
C3 + PC8 &\underset{k_x^{-}}{\overset{k_x^{+}}{\rightleftharpoons}} C3 \cdot PC8 & k_x^{+} &= 10\,\mu\mathrm{M}^{-1}\mathrm{s}^{-1} \\
J_x &= k_x^{+}[C3][PC8] - k_x^{-}[C3 \cdot PC8] & k_x^{-} &= 0.5\,\mathrm{s}^{-1}
\end{aligned}
$$

$$
\begin{aligned}
C3 \cdot PC8 &\xrightarrow{k_x^{f}} C3 + C8 & k_x^{f} &= 0.001\,\mathrm{s}^{-1} \\
J_x^{f} &= k_x^{f}[C3 \cdot PC8]
\end{aligned}
$$

Cleavage of Bid by caspase-3 and subsequent translocation to mitochondrial outer membrane:

$$C3 + Bid \rightarrow C3 + tBid_{mito}$$
$$J_8 = \frac{k_8^+(\mu + k_8^f)[C3][Bid]}{mu + k_8^- + k_8^f}$$
$$J_8^f = \frac{k_8^+ k_8^f[C3][Bid]}{mu + k_8^- + k_8^f}$$

Release of AIF from mitochondria to cytoplasm and translocation to nucleus:

$$C3 + AIF_{mito} \xrightarrow{k_{20}} C3 + AIF_{nuc} \qquad k_{20} = 1\,\mu\mathrm{M}^{-1}\mathrm{s}^{-1}$$
$$J_{20} = k_{20}[C3][AIF_{mito}]$$

Activation of DNase by AIF in nucleus:

$$AIF_{nuc} + DNase \rightarrow AIF_{nuc} + DNase_{active}$$
$$J_{22} = \frac{k_{22}^+(\mu + k_{22}^f)[AIF_{nuc}][DNase]}{mu + k_{22}^- + k_{22}^f}$$

Fragmentation of DNA by active DNase:

$$DNA + DNase_{active} \xrightarrow{k_{23}} DNA + DNA_{damaged} + DNase_{active} \qquad k_{23} = 0.5\,\mu\mathrm{M}^{-1}\mathrm{s}^{-1}$$
$$J_{23} = k_{23} \cdot F([DNA]; \alpha_{23}, \beta_{23}) \cdot [DNase_{active}] \qquad \alpha_{23} = 6, \beta_{23} = 5$$

where function F is a cumulative distribution function of beta distribution with shape parameters α_{23} and β_{23} defined by (5.2).

Activation of CAD by cleaving ICAD in CAD·ICAD complex by active caspase-3, dimerisation and translocation into nucleus:

$$C3 + CAD \cdot ICAD \rightarrow C3 + CAD_{2,nuc}$$
$$J_{24a} = k_{24a}^+[C3][CAD \cdot ICAD]$$
$$J_{24a}^f = k_{24a}^f[CAD \cdot ICAD \cdot C3]$$
$$J_{24b} = k_{24b}^+[C3][CAD \cdot ICAD_{Asp^{224}}]$$
$$J_{24b}^f = k_{24b}^f[CAD \cdot ICAD_{Asp^{224}} \cdot C3]$$

$$J_{25} = k_{25}[CAD][ICAD]$$
$$J_{26} = k_{26}[CAD]^2$$

where

$$[CAD \cdot ICAD \cdot C3] = \frac{k^+_{24a}[CAD \cdot ICAD][C3]}{\mu + k^-_{24a} + k^f_{24a}}$$
$$[CAD \cdot ICAD_{Asp^{224}} \cdot C3] = \frac{k^+_{24b}A[C3]}{\mu - k^+_{24b}B[C3] + k^-_{24b} + k^f_{24b}}$$
$$[CAD \cdot ICAD_{Asp^{224}}] = A + B[CAD \cdot ICAD_{Asp^{224}} \cdot C3]$$
$$[CAD] = \frac{-a_1 + \sqrt{a_1^2 - 4a_2a_0}}{2a_2}$$
$$A = \frac{k^f_{24a}[CAD \cdot ICAD \cdot C3]}{2(\mu + k^+_{24b}[C3])}$$
$$B = \frac{k^-_{24b}}{\mu + k^+_{24b}[C3]}$$
$$a_0 = 0.5 \cdot k^f_{24a}[CAD \cdot ICAD \cdot C3] + k^f_{24b}[CAD \cdot ICAD_{Asp^{224}} \cdot C3]$$
$$a_1 = \mu + k_{25}[ICAD]$$
$$a_2 = 2k_{26}$$

Fragmentation of DNA by nuclear CAD_2 dimer:

$$NA + CAD_{2,nuc} \xrightarrow{k_{29}} DNA + DNA_{damaged} + CAD_{2,nuc} \qquad k_{29} = 0.5\,\mu\mathrm{M}^{-1}\mathrm{s}^{-1}$$
$$J_{29} = k_{29} \cdot \hat{f}\,([DNA]; \alpha_{29}, \beta_{29}) \cdot [CAD_{2,nuc}] \qquad \alpha_{29} = 3, \beta_{29} = 2$$

where function $\hat{f}$ is the probability density function of Beta distribution with shape parameters α_{29} and β_{29} normalised so that the maximum is one and is defined by the (5.4).

Self-repair of DNA:

$$DNA + DNA_{damaged} \xrightarrow{k_{30}} DNA \qquad k_{30} = 0.001\,\mu\mathrm{M}^{-1}\mathrm{s}^{-1}$$
$$J_{30} = k_{30} \cdot \hat{f}([DNA]; \alpha_{30}, \beta_{30}) \qquad \alpha_{30} = 2, \beta_{30} = 10$$

where function $\hat{f}$ is the probability density function of Beta distribution with shape parameters α_{29} and β_{29} normalised so that the maximum is one and is defined by the (5.4).

Reduction of mitochondrial activity by Bax_2 channels:

$$mit + Bax_2 \xrightarrow{k_{31}} mit + mit_{inactive} + Bax_2 \qquad k_{31} = 0.001\,\mathrm{s}^{-1}$$

$$J_{31} = k_{31}\frac{[Bax_2]}{M_{Bax_2}}[mit] \qquad M_{Bax_2} = 0.052\,\mu\mathrm{M}$$

where M_{Bax_2} is the maximal concentration of Bax_2 channels on mitochondrial outer membrane.

Increase in mitochondrial activity in absence of Bax_2 channels:

$$mit + mit_{inactive} \xrightarrow{k_{32}} mit \qquad k_{32} = 0.01\,\mathrm{s}^{-1}$$

$$J_{32} = k_{32}\left(1 - \frac{[Bax_2]}{M_{Bax_2}}\right)(1 - [mit]) \qquad M_{Bax_2} = 0.052\,\mu\mathrm{M}$$

where M_{Bax_2} is the maximal concentration of Bax_2 channels on mitochondrial outer membrane.

Synthesis and degradation of molecules:

$$DNA \xrightarrow{\Omega_{PC8}} PC8 \qquad \Omega_{PC8} = 6 \cdot 10^{-4}\,\mu\mathrm{Ms}^{-1}$$

$$DNA \xrightarrow{\Omega_{Bid}} Bid \qquad \Omega_{Bid} = 6 \cdot 10^{-5}\,\mu\mathrm{Ms}^{-1}$$

$$DNA \xrightarrow{\Omega_{Bax}} Bax \qquad \Omega_{Bax} = 5 \cdot 10^{-4}\,\mu\mathrm{Ms}^{-1}$$

$$mit \xrightarrow{\Omega_{c_{mito}}} c_{mito} \qquad \Omega_{c_{mito}} = 5 \cdot 10^{-4}\,\mu\mathrm{Ms}^{-1}$$

$$DNA \xrightarrow{\Omega_{Apaf\text{-}1}} Apaf\text{-}1 \qquad \Omega_{Apaf\text{-}1} = 6 \cdot 10^{-4}\,\mu\mathrm{Ms}^{-1}$$

$$DNA \xrightarrow{\Omega_{PC9}} PC9 \qquad \Omega_{PC9} = 6 \cdot 10^{-4}\,\mu\mathrm{Ms}^{-1}$$

$$DNA \xrightarrow{\Omega_{PC3}} PC3 \qquad \Omega_{PC3} = 6 \cdot 10^{-4}\,\mu\mathrm{Ms}^{-1}$$

$$mit \xrightarrow{\Omega_{AIF_{mito}}} AIF_{mito} \qquad \Omega_{AIF_{mito}} = 3 \cdot 10^{-4}\,\mu\mathrm{Ms}^{-1}$$

$$DNA \xrightarrow{\Omega_{DNase}} DNase \qquad \Omega_{DNase} = 5 \cdot 10^{-5}\,\mu\mathrm{Ms}^{-1}$$

$$DNA \xrightarrow{\Omega_{ICAD}} ICAD \qquad \Omega_{ICAD} = 6 \cdot 10^{-4}\,\mu\mathrm{Ms}^{-1}$$

$$DNA + ICAD \xrightarrow{\Omega_{CAD}} CAD \cdot ICAD \qquad \Omega_{CAD} = 6 \cdot 10^{-4}\,\mathrm{s}^{-1}$$

Conclusion

In this thesis we studied two mathematical models proposed in [23]. After detailed study of the relevant biological literature we were able to propose several modifications, derive different, biologically more viable mitochondrial dynamics and expand model proposed in [23, Chapter 4] to include DNA fragmentation occurring during apoptosis and its effect on synthesis of proteins involved in apoptotical machinery in order to increase biological accuracy and relevance of the proposed models.

We verified the analysis of the steady states of reduced model and showed that the results for model with the proposed modifications are qualitatively the same as for the model without modifications. Also we were able to derive upper bound on concentration of cytochrome c in cytoplasm in steady state.

Then we showed that mathematical model proposed in [23, Chapter 4] with slight biologically motivated modifications displays a bistable behaviour in response to strength of the initial apoptotic signal that was observed in experiments. The sensitivity analysis of parameters associated with the influence of Trichinella spiralis on apoptosis was conducted to gain insight into possible mechanisms by which Trichinella can regulate apoptosis.

We challenged assumption about the influence of Trichinella spiralis after an invasion into a muscle cell and proposed hypothesis that Trichinella triggers apoptosis to damage the muscle cell and subsequently hijacks repair machinery of muscle cell to facilitate nurse cell formation that takes into account experimentally observed mitochondrial dynamics during apoptosis and structure of muscle cells. We modified the model accordingly and also expanded it to incorporate the reactions involved in apoptotic DNA fragmentation.

Finally we were able to significantly reduce the dimension of the system of differential equations describing the proposed expanded model of apoptosis while preserving the qualitative behaviour of the system.

In addition to the reduction performed in this thesis it may be possible to introduce a further reduction of the model. The eventual opportunities may lie in an approximation of the concentration of active $DNase$ by an appropriate multiple of the concentration of nuclearly localised AIF as evolutions of their concentrations appear to go hand in hand.

Also there are parts that were modelled only phenomenologically, i.e. mitochondrial dynamics and DNA fagmentation, and need more investigation.

References

[1] Devrim Acehan, Xuejun Jiang, David Gene Morgan, John E Heuser, Xiaodong Wang, and Christopher W Akey. Three-dimensional structure of the apoptosome: implications for assembly, procaspase-9 binding, and activation. *Molecular cell*, 9(2):423–432, 2002.

[2] Peter J Adhihetty, Michael FN O'Leary, and David A Hood. Mitochondria in skeletal muscle: adaptable rheostats of apoptotic susceptibility. *Exercise and sport sciences reviews*, 36(3):116–121, 2008.

[3] Bruno Antonsson, Franco Conti, AnnaMaria Ciavatta, Sylvie Montessuit, Shareta Lewis, Isabelle Martinou, Lilia Bernasconi, Alain Bernard, Jean-Jacques Mermod, Gonzalo Mazzei, et al. Inhibition of bax channel-forming activity by bcl-2. *Science*, 277(5324):370–372, 1997.

[4] Damien Arnoult, Brigitte Gaume, Mariusz Karbowski, Juanita C Sharpe, Francesco Cecconi, and Richard J Youle. Mitochondrial release of aif and endog requires caspase activation downstream of bax/bak-mediated permeabilization. *The EMBO Journal*, 22(17):4385–4399, 2003.

[5] Pavel Babal, Rosica Milcheva, Svetlozara Petkova, Pavol Janega, and Zuzana Hurnikova. Apoptosis as the adaptation mechanism in survival of trichinella spiralis in the host. *Parasitology research*, 109(4):997–1002, 2011.

[6] Elife Zerrin Bagci. *Mathematical modeling and simulation of apoptosis and nitric oxide effects*. ProQuest, 2007.

[7] M Bentele, I Lavrik, M Ulrich, S Stösser, DW Heermann, H Kalthoff, PH Krammer, and R Eils. Mathematical modeling reveals threshold mechanism in cd95-induced apoptosis. *The Journal of cell biology*, 166(6):839–851, 2004.

[8] T Boonmars, Z Wu, I Nagano, and Y Takahashi. Expression of apoptosis-related factors in muscles infected with trichinella spiralis. *Parasitology*, 128(03):323–332, 2004.

[9] Hsiuchen Chen, Scott A Detmer, Andrew J Ewald, Erik E Griffin, Scott E Fraser, and David C Chan. Mitofusins mfn1 and mfn2 coordinately regulate mitochondrial fusion and are essential for embryonic development. *The Journal of cell biology*, 160(2):189–200, 2003.

[10] Solange Desagher and Jean-Claude Martinou. Mitochondria as the central control point of apoptosis. *Trends in cell biology*, 10(9):369–377, 2000.

[11] Solange Desagher, Astrid Osen-Sand, Anthony Nichols, Robert Eskes, Sylvie Montessuit, Sandra Lauper, Kinsey Maundrell, Bruno Antonsson, and Jean-Claude Martinou. Bid-induced conformational change of bax is responsible for mitochondrial cytochrome c release during apoptosis. *The Journal of cell biology*, 144(5):891–901, 1999.

[12] DD Despommier. How does trichinella spiralis make itself at home? *Parasitology Today*, 14(8):318–323, 1998.

[13] Zheng Dong, Pothana Saikumar, Joel M Weinberg, and Manjeri A Venkatachalam. Internucleosomal dna cleavage triggered by plasma membrane damage during necrotic cell death. involvement of serine but not cysteine proteases. *The American journal of pathology*, 151(5):1205, 1997.

[14] Frank Edlich, Soojay Banerjee, Motoshi Suzuki, Megan M Cleland, Damien Arnoult, Chunxin Wang, Albert Neutzner, Nico Tjandra, and Richard J Youle. Bcl-x l retrotranslocates bax from the mitochondria into the cytosol. *Cell*, 145(1):104–116, 2011.

[15] Thomas Eissing, Holger Conzelmann, Ernst D Gilles, Frank Allgöwer, Eric Bullinger, and Peter Scheurich. Bistability analyses of a caspase activation model for receptor-induced apoptosis. *Journal of Biological Chemistry*, 279(35):36892–36897, 2004.

[16] Masato Enari, Hideki Sakahira, Hideki Yokoyama, Katsuya Okawa, Akihiro Iwamatsu, and Shigekazu Nagata. A caspase-activated dnase that degrades dna during apoptosis, and its inhibitor icad. *Nature*, 391(6662):43–50, 1998.

[17] Martin Fussenegger, James E Bailey, and Jeffrey Varner. A mathematical model of caspase function in apoptosis. *Nature biotechnology*, 18(7):768–774, 2000.

[18] Atan Gross, Xiao-Ming Yin, Kun Wang, Michael C Wei, Jennifer Jockel, Curt Milliman, Hediye Erdjument-Bromage, Paul Tempst, and Stanley J Korsmeyer. Caspase cleaved bid targets mitochondria and is required for cytochrome c release, while bcl-xl prevents this release but not tumor necrosis factor-r1/fas death. *Journal of Biological Chemistry*, 274(2):1156–1163, 1999.

[19] Ji-Young Hong, Geun-Hong Kim, Jun-Woo Kim, Soon-Sung Kwon, Eisuke F Sato, Kwang-Hyun Cho, and Eun Bo Shim. Computational modeling of apoptotic signaling pathways induced by cisplatin. *BMC systems biology*, 6(1):1, 2012.

[20] Chahrazade Kantari and Henning Walczak. Caspase-8 and bid: caught in the act between death receptors and mitochondria. *Biochimica et Biophysica Acta (BBA)-Molecular Cell Research*, 1813(4):558–563, 2011.

[21] Hyungjin Kim, Ho-Chou Tu, Decheng Ren, Osamu Takeuchi, John R Jeffers, Gerard P Zambetti, James J-D Hsieh, and Emily H-Y Cheng. Stepwise activation of bax and bak by tbid, bim, and puma initiates mitochondrial apoptosis. *Molecular cell*, 36(3):487–499, 2009.

[22] Young-Myeong Kim, Tae-Hyoung Kim, Dai-Wu Seol, Robert V Talanian, and Timothy R Billiar. Nitric oxide suppression of apoptosis occurs in association with an inhibition of bcl-2 cleavage and cytochrome crelease. *Journal of Biological Chemistry*, 273(47):31437–31441, 1998.

[23] Jakub Kovacs. Mathematical modelling of cell death in presence of synchronous invasion of trichinella spiralis parasite. Master's thesis, Faculty of mathematics, physics and informatics, Comenius University, 2014.

[24] Stefan Legewie, Nils Blüthgen, and Hanspeter Herzel. Mathematical modeling identifies inhibitors of apoptosis as mediators of positive feedback and bistability. *PLoS Comput Biol*, 2(9):e120, 2006.

[25] Honglin Li, Hong Zhu, Chi-jie Xu, and Junying Yuan. Cleavage of bid by caspase 8 mediates the mitochondrial damage in the fas pathway of apoptosis. *Cell*, 94(4):491–501, 1998.

[26] Xuesong Liu, Peng Li, Piotr Widlak, Hua Zou, Xu Luo, William T Garrard, and Xiaodong Wang. The 40-kda subunit of dna fragmentation factor induces dna fragmentation and chromatin condensation during apoptosis. *Proceedings of the National Academy of Sciences*, 95(15):8461–8466, 1998.

[27] Xu Luo, Imawati Budihardjo, Hua Zou, Clive Slaughter, and Xiaodong Wang. Bid, a bcl2 interacting protein, mediates cytochrome c release from mitochondria in response to activation of cell surface death receptors. *Cell*, 94(4):481–490, 1998.

[28] Michael Lutter, Guy A Perkins, and Xiaodong Wang. The pro-apoptotic bcl-2 family member tbid localizes to mitochondrial contact sites. *BMC cell biology*, 2(1):1, 2001.

[29] Shigekazu Nagata. Apoptosis by death factor. *cell*, 88(3):355–365, 1997.

[30] Stefan J Riedl, Wenyu Li, Yang Chao, Robert Schwarzenbacher, and Yigong Shi. Structure of the apoptotic protease-activating factor 1 bound to adp. *Nature*, 434(7035):926–933, 2005.

[31] Joe Rodriguez and Yuri Lazebnik. Caspase-9 and apaf-1 form an active holoenzyme. *Genes & development*, 13(24):3179–3184, 1999.

[32] Guy S Salvesen and Colin S Duckett. Iap proteins: blocking the road to death's door. *Nature reviews Molecular cell biology*, 3(6):401–410, 2002.

[33] Clare Sheridan, Petrina Delivani, Sean P Cullen, and Seamus J Martin. Bax-or bak-induced mitochondrial fission can be uncoupled from cytochrome c release. *Molecular cell*, 31(4):570–585, 2008.

[34] Eric N Shiozaki, Jijie Chai, Daniel J Rigotti, Stefan J Riedl, Pingwei Li, Srinivasa M Srinivasula, Emad S Alnemri, Robert Fairman, and Yigong Shi. Mechanism of xiap-mediated inhibition of caspase-9. *Molecular cell*, 11(2):519–527, 2003.

[35] Elizabeth A Slee, Sinéad A Keogh, and Seamus J Martin. Cleavage of bid during cytotoxic drug and uv radiation-induced apoptosis occurs downstream of the point of bcl-2 action and is catalysed by caspase-3: a potential feedback loop for amplification of apoptosis-associated mitochondrial cytochrome c release. 2000.

[36] Alexander H Stegh, Bryan C Barnhart, Jörg Volkland, Alicia Algeciras-Schimnich, Ning Ke, John C Reed, and Marcus E Peter. Inactivation of caspase-8 on mitochondria of bcl-xl-expressing mcf7-fas cells role for the bifunctional apoptosis regulator protein. *Journal of Biological Chemistry*, 277(6):4351–4360, 2002.

[37] Santos A Susin, Hans K Lorenzo, Naoufal Zamzami, Isabel Marzo, Bryan E Snow, Greg M Brothers, Joan Mangion, Etienne Jacotot, Paola Costantini, Markus Loeffler, et al. Molecular characterization of mitochondrial apoptosis-inducing factor. *Nature*, 397(6718):441–446, 1999.

[38] György Szabadkai, Anna Maria Simoni, Mounia Chami, Mariusz R Wieckowski, Richard J Youle, and Rosario Rizzuto. Drp-1-dependent division of the mitochondrial network blocks intraorganellar ca 2+ waves and protects against ca 2+-mediated apoptosis. *Molecular cell*, 16(1):59–68, 2004.

[39] Xiaodong Wang. The expanding role of mitochondria in apoptosis. *Genes & development*, 15(22):2922–2933, 2001.

[40] Michael C Wei, Wei-Xing Zong, Emily H-Y Cheng, Tullia Lindsten, Vily Panoutsakopoulou, Andrea J Ross, Kevin A Roth, Grant R MacGregor, Craig B Thompson, and Stanley J Korsmeyer. Proapoptotic bax and bak: a requisite gateway to mitochondrial dysfunction and death. *Science*, 292(5517):727–730, 2001.

[41] Keith G Wolter, Yi-Te Hsu, Carolyn L Smith, Amotz Nechushtan, Xu-Guang Xi, and Richard J Youle. Movement of bax from the cytosol to mitochondria during apoptosis. *The Journal of cell biology*, 139(5):1281–1292, 1997.

[42] Eui-Jeon Woo, Yeon-Gil Kim, Min-Sung Kim, Won-Deok Han, Sejeong Shin, Howard Robinson, Sam-Yong Park, and Byung-Ha Oh. Structural mechanism for inactivation and activation of cad/dff40 in the apoptotic pathway. *Molecular cell*, 14(4):531–539, 2004.

[43] Zhiliang Wu, Lj Sofronic-Milosavljevic, Isao Nagano, and Yuzo Takahashi. Trichinella spiralis: nurse cell formation with emphasis on analogy to muscle cell repair. *Parasit Vectors*, 1(1):27, 2008.

[44] Shujun Yuan and Christopher W Akey. Apoptosome structure, assembly, and procaspase activation. *Structure*, 21(4):501–515, 2013.

[45] Victor J Yuste, Isabel Sánchez-López, Carme Solé, Rana S Moubarak, José R Bayascas, Xavier Dolcet, Mario Encinas, Santos A Susin, and Joan X Comella. The contribution of apoptosis-inducing factor, caspase-activated dnase, and inhibitor of caspase-activated dnase to the nuclear phenotype and dna degradation during apoptosis. *Journal of Biological Chemistry*, 280(42):35670–35683, 2005.

[46] Hong Zhang, Qunli Xu, Stanislaw Krajewski, Maryla Krajewska, Zhihua Xie, Sally Fuess, Shinichi Kitada, Krzysztof Pawłowski, Adam Godzik, and John C Reed. Bar: An apoptosis regulator at the intersection of caspases and bcl-2 family proteins. *Proceedings of the National Academy of Sciences*, 97(6):2597–2602, 2000.

[47] Hua Zou, Yuchen Li, Xuesong Liu, and Xiaodong Wang. An apaf-1· cytochrome c multimeric complex is a functional apoptosome that activates procaspase-9. *Journal of Biological Chemistry*, 274(17):11549–11556, 1999.